

A photometric and spectroscopic study of dwarf and giant galaxies in the Coma cluster –

III. Spectral ages and metallicities ¹

Bianca M. Poggianti,² Terry J. Bridges,³ Bahram Mobasher,⁴ Dave Carter,⁵ M. Doi,⁶ M. Iye,⁷ N. Kashikawa,⁷ Y. Komiyama,⁸ S. Okamura,^{9,11} M. Sekiguchi,¹⁰ K. Shimasaku,⁹ M. Yagi,⁷ N. Yasuda⁷

2) Osservatorio Astronomico di Padova, vicolo dell'Osservatorio 5, 35122 Padova, Italy

3) Anglo-Australian Observatory, PO Box 296, Epping, NSW 1710, Australia

4) Space Telescope Science Institute, 3700 San Martin Drive, Baltimore, MD 21218, USA

Affiliated with the Space Sciences Department of the European Space Agency

5) Liverpool John Moores University, Astrophysics Research Institute, Twelve Quays House, Egerton Wharf, Birkenhead, Wirral, CH41 1LD, UK

6) Institute of Astronomy, School of Science, University of Tokyo, Mitaka, 181-0015, Japan

7) National Astronomical Observatory, Mitaka, Tokyo, 181-8588 Japan

8) Subaru Telescope, 650 North Aohoku Place, Hilo, HI 96720, USA

9) Department of Astronomy, University of Tokyo, Bunkyo-ku, Tokyo 113-0033, Japan

10) Institute for Cosmic Ray Research, University of Tokyo, Kashiwa, Chiba 277-8582, Japan

11) Research Center for the Early Universe, School of Science, University of Tokyo, Tokyo 113-0033, Japan

ABSTRACT

We present a detailed analysis of the spectroscopic catalog of galaxies in the Coma cluster from Mobasher et al. (2001, Paper II of the series). This catalog comprises ~ 300 spectra of cluster members with absolute magnitudes in the range $M_B = -20.5$ to -14 in two areas of $\sim 1 \times 1.5$ Mpc towards the center and the South-West region of the cluster. In order to study the star formation and metallicity properties of the Coma galaxies as a function of their luminosity and environment, spectral indices of the Lick/IDS system and equivalent widths of the emission lines were measured in the range $\lambda = 3600 - 6600$ Å.

In this paper the analysis is restricted to the 257 galaxies with no emission lines in their spectra. The strength of the age-sensitive indices (such as $H\beta$, $H\gamma_F$ and $H\delta_F$) is found to correlate with galaxy magnitude over the whole magnitude range explored in this study. Similarly, the metallicity-sensitive indices (such as Mg_2 , $\langle Fe \rangle$, C_{24668}) anticorrelate with magnitude. By comparing the observed indices with model grids based on the Padova isochrones, we derive luminosity-weighted ages and metallicities. We present the distributions of ages and metallicities for galaxies in various magnitude bins. The mean metallicity decreases with galaxy magnitude and, at a given luminosity, appears to be generally lower for galaxies in the South-West region of Coma as compared to the center of the cluster. A broad range of ages, from younger than 3 Gyr to older than 9 Gyr, is found in galaxies of any magnitude. However, systematic trends of age with luminosity are present among galaxies in the central field, including a slight decrease of the mean age for fainter galaxies. Furthermore, in the central Mpc of Coma, a large fraction of galaxies at *any* luminosity (50 – 60% of the giants, > 30% of the dwarfs) show no evidence in their central regions of star formation occurred

¹Based on observations made with the William Herschel Telescope operated on the island of La Palma by the Isaac Newton Group in the Spanish Observatorio del Roque de los Muchachos of the Instituto de Astrofísica de Canarias.

at redshift $z < 2$, while the proportion of galaxies with significant star formation occurring at intermediate ($0.35 < z < 2$) and low ($z < 0.35$) redshifts is found to depend on galaxy luminosity.

An additional surprising result is that the faint galaxies with young luminosity-weighted ages appear to have a bimodal metallicity distribution that, if confirmed, would point to a composite formation scenario involving different physical processes. Coadding the spectra of these metal-rich and metal-poor galaxies separately supports the reality of the metallicity bimodality, although higher signal-to-noise spectra of the individual galaxies will be needed to draw definite conclusions.

An anticorrelation between age and metallicity is found to be present in galaxies of any given luminosity bin and it is especially evident among the brightest subset with the highest signal-to-noise spectra.

Finally, we present an interpretation of the index-magnitude relations observed. We show that the slopes of the indices/magnitude relations are the consequence of both age and metallicity trends with luminosity: each such trend on its own would be sufficient to produce relations similar to those observed.

Subject headings:

Received _____; accepted _____

1. Introduction

Dwarf galaxies are the most numerous type of galaxy in the local Universe. In hierarchical models, they represent the “building blocks” of more massive galaxies, and are expected to be the sites of the earliest cosmic star formation (White & Frenk 1991). Their observed numbers and properties at various redshifts are a strong test of any theory of galaxy formation and evolution.

Furthermore, dwarfs are expected to be the type of galaxies that can best teach us the influence of both internal and external conditions on galaxy evolution. Their structures and evolutionary histories are predicted to be strongly affected by mass loss due to supernova-driven outflows (Larson 1974, Dekel & Silk 1986, Silk, Wyse & Shields 1987), and their star formation is expected to be modulated also by the external UV radiation field (Babul & Rees 1992, Efstathiou 1992).

Dwarf galaxies are influenced by environment even more than giant galaxies are. Dwarfs show the strongest morphology-density relation: early-type dwarfs are found in clusters or clustered around giant galaxies, while late-type dwarfs are the least clustered type of galaxy. In the Local Group, this morphological segregation could be induced by the repeated action of tidal forces from the closest giant galaxy (“tidal stirring”, Mayer et al. 2000). In clusters like Coma, physical processes peculiar to dense environments such as interactions with a hot intracluster medium via pressure confinement, shocks or ram pressure stripping (Silk, Wyse & Shields 1987, Babul & Rees 1992, Murakami & Babul 1999) and high-speed, repeated encounters (“harassment”, Moore et al. 1996, 1998) are expected to have the most dramatic effects on the dwarfs. Many of the suggested processes imply a morphological evolution from one dwarf type to another (early-type to late-type dwarfs and vice-versa).

Surprisingly little is known about the stellar populations of non-starforming dwarf galaxies. The two environments where such low luminosity galaxies have been identified in significant numbers are the Local Group and other groups and clusters of galaxies. By far the best studied environment in this respect is the Local Group, where non-starforming dwarfs show evidence of varied and complex histories, sometimes with multiple episodes of star formation (Mateo 1998, Grebel 1999). In fact, they vary widely in the star formation rate, the length and the epoch of star formation episodes and the chemical enrichment *even within the same morphological class*: “no two dwarf galaxies in the LG have the same star formation history” (Grebel 1999). Regardless of this variety of evolutionary histories, the Local Group dwarf galaxies follow global relations between absolute magnitude, mean metallicity and central surface brightness (Caldwell 1999, Grebel & Guhathakurta 1999). Interestingly, dwarf galaxy evolution in the Local Group appears to be determined both by mass and by environmental effects (i.e. proximity to a massive spiral) (Grebel 2000).

Spectroscopic studies of non-starforming dwarf galaxies outside the Local Group have been limited so far to quite small samples, thus it is still largely unknown whether low-luminosity cluster galaxies share the diversity of star formation histories of dwarfs in the Local Group, and whether they follow a similar metallicity-luminosity relation. A metallicity-luminosity relation valid for both bright and dwarf ellipticals (the latter residing mostly in the Virgo and Fornax clusters) over the range $M_B = -14$ to -22 was presented by Brodie & Huchra (1991), who also noted that the scatter in this relation implies that additional parameters are involved. Interestingly, ten dwarf ellipticals in the Fornax cluster were found to cover a wide range of metallicities *at a given luminosity* (Held & Mould 1994).

Broadband photometry first provided evidence for young or intermediate age populations in some dwarf ellipticals (Caldwell 1983, Thuan 1985, Caldwell & Bothun 1987), and the poor correlation between the UBV colors and the structural parameters was interpreted by Peterson & Caldwell (1993) as evidence for

variations in the ages of dwarf ellipticals. Early spectroscopic studies of bright dwarf ellipticals/spheroidals supported the photometric indications for young or intermediate-age stellar populations in some of the dwarfs (Zinnecker et al. 1985, Bothun & Mould 1988, Gregg 1991, Held & Mould 1994). Recently, six spheroidals in Virgo ($M_B = -17/-18$) have been studied by Gorgas et al. (1997), who analyzed their Lick indices and found four of them to be old and quite metal-poor ($[\text{Fe}/\text{H}] \sim -0.75$) and two of them to be young and metal-rich. Recent star formation in a fraction of the early-type galaxies has been detected in Coma and other clusters (Caldwell et al. 1993, Caldwell & Rose 1997, Caldwell & Rose 1998), most of these galaxies being fainter than $M_B = -18.5$.

There are now several pieces of evidence indicating that the spread in the average stellar ages of *low-luminosity* early-type galaxies in all environments is larger than the age spread of the *luminous* early-type galaxies (Bender, Burstein & Faber 1993; Bressan et al. 1996; Worthey 1997; Worthey 1998; Kuntschner & Davies 1998; Mehlert et al. 1998; Vazdekis & Arimoto 1999; Smail et al. 2001). In the Coma cluster, the scatter in age and metallicity has been found to increase with decreasing mass/luminosity (Jorgensen 1999). Concannon, Rose & Caldwell (2000) analyzed the index-velocity dispersion relation for Mg_2 , $\text{H}\beta$ and a Rose index of field and cluster E/S0 galaxies with a large magnitude range ($M_B = -22$ to -16) and found for all three indices a relation whose scatter is greater for lower mass galaxies. Their interpretation of this result is that less massive galaxies have experienced a more varied SF history and the spread in age increases towards lower velocity dispersions.

We are still far from a full understanding of the meaning of these findings and their implications for theories of galaxy formation and evolution. The scarcity of information and the lack of systematic studies regarding the evolutionary histories of dwarf galaxies external to the Local group has hindered a detailed comparison with the giant galaxies, whose ages and metallicities have been investigated by a large number of studies. Tight relations between the strength of the Mg-absorption and the central velocity dispersion (or luminosity) has long been known to exist for luminous early-type galaxies (Faber 1973; Terlevich et al. 1981; Dressler 1984; Dressler et al. 1987; Burstein et al. 1988; Guzman et al. 1992; Bender, Burstein & Faber 1993; Jorgensen, Franx & Kjaergaard 1996; Bender, Ziegler & Bruzual 1996; Ziegler & Bender 1997; Bender et al. 1998; Trager et al. 1998; Colless et al. 1999; Kuntschner et al. 2001). Correlations of other metal line indices with velocity dispersion/luminosity have generally been found to be weak and to have a large scatter (Fisher, Franx & Illingworth 1996; Jorgensen 1997, 1999; Trager et al. 1998; Terlevich et al. 1999). Recently, strong, significant correlations of metal indices other than magnesium with velocity dispersion were measured in a sample of early-type galaxies in the Fornax cluster (Kuntschner 2000; Kuntschner et al. 2001). Negative correlations of Balmer indices with the velocity dispersion or luminosity have also been reported by a number of authors (González 1993; Jorgensen 1997; Trager et al. 1998; Terlevich et al. 1999; Kuntschner 2000). Shell and pair galaxies are known to deviate from the $\text{H}\beta - \sigma$ (both shell and pair galaxies) and the $\text{Mg}_2 - \sigma$ (only shell galaxies) relations, most likely due to secondary bursts of star formation (Longhetti et al. 2000).

The relations observed in luminous early-type galaxies have generally been interpreted to be largely a sequence of metallicity versus galaxy mass/luminosity (Forbes et al. 1998; Kobayashi & Arimoto 1999; Terlevich et al. 1999; Kuntschner 2000; Kuntschner et al. 2001), although an issue still debated is whether the observed trends are entirely due to a metallicity sequence or to a combination of both age and metallicity effects (e.g. Jorgensen 1999, Trager et al. 2000b). The most controversial issue in these studies are the star formation histories of the early-type galaxies. Ellipticals in the Fornax cluster are mostly coeval and span a range in metallicity (Kuntschner & Davies 1998; Kuntschner 2000). Similarly, a new sample of early-type galaxies in cluster and group environments consists mostly of galaxies with large ages

spanning a range in metallicity (Kuntschner et al. 2001). In contrast, intermediate-age/young populations have been found in a large fraction of non-cluster luminous ellipticals (Rose 1985; González 1993; Forbes, Ponman & Brown 1998). The González dataset has been analyzed by a number of authors, all agreeing on the existence of a large age spread in this sample (Faber et al. 1995; Bressan et al. 1996; Tantalo et al. 1998; Kuntschner & Davies 1998; Trager et al. 2000a), except Maraston & Thomas (2000) who argue that the $H\beta$ index of the majority of galaxies in the González sample (excluding the Balmer-strong lenticulars, intermediate-mass field ellipticals and dwarf ellipticals) can be explained by a spread in the metallicity of old stellar populations.

The different age ranges found in different samples of ellipticals might be due to systematic effects as a function of environment, with ellipticals in dense environments being older than those in groups and in the field (Bower et al. 1990; Guzman et al. 1992; de Carvalho & Djorgovski 1992; Rose et al. 1994; Jorgensen 1997; Kauffmann & Charlot 1998; Kuntschner & Davies 1998; Mobasher & James 2000; Trager et al. 2000b), although a large age spread has also been found by Jorgensen (1999) in Coma E and S0 galaxies spanning a 5 magnitude range. On the other hand, the luminosity-dependence of the galactic properties has not been clarified yet. As will be demonstrated by the present work, it is only meaningful to compare galaxies of *similar luminosity/mass*. At least part of the differences observed in the various datasets could be due to differences in the luminosity range explored.

In addition, it is important to ask to what extent the star formation history of a non-starforming galaxy is related to its Hubble type. In the Fornax cluster, luminous ellipticals are coeval (around 8 Gyr), while (less luminous) S0 galaxies display a significant age spread (Kuntschner & Davies 1998; Kuntschner 2000). In apparent contrast, Jorgensen (1999) finds no difference between the stellar population properties of bright E’s and S0’s in Coma, and a similar result is obtained for clusters at $z=0.3-0.5$ by Jones, Smail & Couch (2000). These results could be simultaneously interpreted if the dependence of galaxy age on morphology is relevant only for non-luminous galaxies, as highlighted by the work of Smail et al. (2001) who find that ellipticals of all magnitudes and luminous S0s in the cluster A2218 at $z=0.17$ are coeval and trace a sequence of varying metallicity, while faint S0 galaxies span a large range of luminosity-weighted ages.

Obviously a key issue is understanding the relative roles of galaxy mass (=luminosity, assuming an approximately constant stellar mass-to-light ratio as for old populations), environmental conditions, and galaxy morphology, in determining the evolutionary history of galaxies. This project aims at investigating how many and which parameters govern the evolution of low- and high-luminosity cluster galaxies, by obtaining photometric and spectroscopic information for galaxies in the Coma cluster. For this purpose, the most valuable aspects of the present survey are the large number of spectra, the broad magnitude range covered, the diversity of environmental conditions surveyed and the wide spectral coverage. This is the largest spectroscopic survey of cluster dwarfs currently available and it is complemented by a similarly large dataset for brighter galaxies up to $M_B \sim -20.5$. Given the paucity of spectroscopic studies of low-luminosity cluster galaxies, in a sense we are venturing into an unexplored realm. The survey extends over more than 6 magnitudes, therefore providing an excellent opportunity to study the spectroscopic properties as a function of galaxy luminosity in a homogeneous dataset. Two wide areas of $\sim 1 \times 1.5$ Mpc each (toward the center and in the South-West region of the Coma cluster) were chosen, to encompass very different environmental conditions in terms of local galaxy density, distance from the cluster center, and membership in a substructure. The wavelength range of the spectra ($\sim 3600 - 6600$ Å) includes numerous absorption and emission features, typically from $[OII]\lambda 3727$ to $H\alpha$, hence it offers the chance to use several age and metallicity indicators.

The main goal of this paper (Paper III of the series) is to study the stellar population properties, deriving luminosity-weighted ages and metallicities from the observed spectral indices. After a brief description of the spectroscopic catalog (§2) and of the models employed (§3), we show the relations between the strength of the spectral indices and galaxy luminosity (§4.1), we derive luminosity-weighted ages and metallicities from index-index diagrams (§4.2 and 4.3) and we present the age and metallicity distributions as a function of galaxy magnitude, deriving the proportion of actively starforming galaxies at various redshifts (§4.3). The link between age and metallicity is discussed in §4.4 and §4.5, and in §4.6 we show how the observed index-magnitude relations are a consequence of the systematic variations of age and metallicity with luminosity. A summary of the main results can be found in §5.

2. Sample and spectral analysis

We have carried out a spectroscopic survey of faint and bright galaxies in two fields (each of size $32.5 \times 50.8 \text{ arcmin}^2$) in the direction of the center of the Coma cluster (Coma1), and in the south-west region (Coma3). The coordinates and extent of these fields are presented in Mobasher et al. (2001, Paper II). These areas were imaged in the B and R bands with the Japanese mosaic CCD camera on the William Herschel Telescope (Komiya et al. 2001, Paper I). A full description of the selection of the spectroscopic targets, observations and data reduction can be found in Mobasher et al. (Paper II). Here we only summarize the most important characteristics of the sample and the data.

The spectra were taken with the WYFFOS multi-fibre spectrograph at the William Herschel Telescope. They are centered on 5100 \AA and extend over more than 3000 \AA with a resolution $6 - 9 \text{ \AA FWHM}$ (see Appendix A, dispersion $\sim 3 \text{ \AA/pixel}$). Each fibre has a diameter of 2.7 arcsec , thus the spectra are sampling the central 1.3 kpc of each galaxy ($H_0 = 65 \text{ km s}^{-1} \text{ Mpc}^{-1}$). For comparison, typical exponential scalelengths of dwarf galaxies are in the range $0.8 - 1.3 \text{ kpc}$ for $M_B = -15$ to -17 (Ferguson & Binggeli 1994).

In this paper we restrict our analysis to galaxies with velocities in the range $4000 < v < 10000 \text{ km s}^{-1}$ (roughly corresponding to 3σ cuts), which are considered members of the Coma cluster. With this membership criterion, our spectroscopic catalog comprises a total of 278 galaxies, of which 189 are in Coma1 and 89 in Coma3. The R magnitude distributions of Coma members are presented in Fig. 1 for the Coma1 and the Coma3 fields separately. This survey extends over more than 6 magnitudes, corresponding to a B band absolute magnitude in the range $M_B \sim -20.5$ to -14 mag (the distance modulus adopted is 35.16). For convenience, in the following we will sometimes refer to “dwarf” and “giant” galaxies adopting a threshold $R_{3Kr} = 16.3^2$ corresponding approximately to $M_B = -17.3$; this magnitude limit is expected to separate dwarf galaxies and low-luminosity ellipticals from spiral galaxies and giant ellipticals in most cases (Ferguson & Binggeli 1994). Nevertheless, we stress that this division should only be considered a way to separate the bright and the faint subsamples and does not provide information about any other galactic characteristic such as morphological type or central surface brightness. According to our adopted division, the spectroscopic catalog comprises 160 dwarf and 118 giant galaxies.

²Magnitude over an aperture of radius 3 times the Kron radius. Throughout the paper, $R = R_{3Kr}$.

The selection criteria of the spectroscopic targets were different for the faintest and brightest subsets ($R > 17$ and $R < 17$). At the bright end, the only criterion was membership in the Coma cluster, as already established by previous spectroscopic studies in the literature. At the faint end, a color criterion ($B - R > 1$) was adopted; with this color cut, only the most extreme starburst galaxies will be excluded from the sample. The majority of the faint objects were selected to satisfy $B - R < 2$ (0.5 mag redder than the mean color-magnitude sequence), but a sample was also constructed with redder galaxies to verify that the red color cut did not exclude a significant number of cluster members. A full description of the selection criteria can be found in Paper II (Mobasher et al. 2001).

In order to study the star formation (SF) and metallicity properties of the Coma galaxies as a function of their luminosity and environment, spectral indices and equivalent widths of the main lines were measured. Two types of measurements were performed: the indices of the Lick/IDS system and the strength of eventual emission lines. Furthermore all spectra were classified according to the spectral classification scheme developed by the MORPHS group (Dressler et al. 1999). The Lick indices are employed in this paper to determine the luminosity-weighted abundances and ages in spectra without emission lines (257 Coma galaxies). We stress that this is a *spectroscopic* criterion (only considering non-emission-line galaxies), while no *morphological* criterion was applied. Hence the sample employed in this paper can and *probably is* composed of galaxies of different Hubble types, presumably ellipticals and S0s but possibly also passive, non-starforming spirals such as those observed in distant clusters (Poggianti et al. 1999). The properties of the galaxies with emission-line spectra (21 cluster members in total) and the results of the MORPHS spectral classification will be dealt with in future papers of the series.

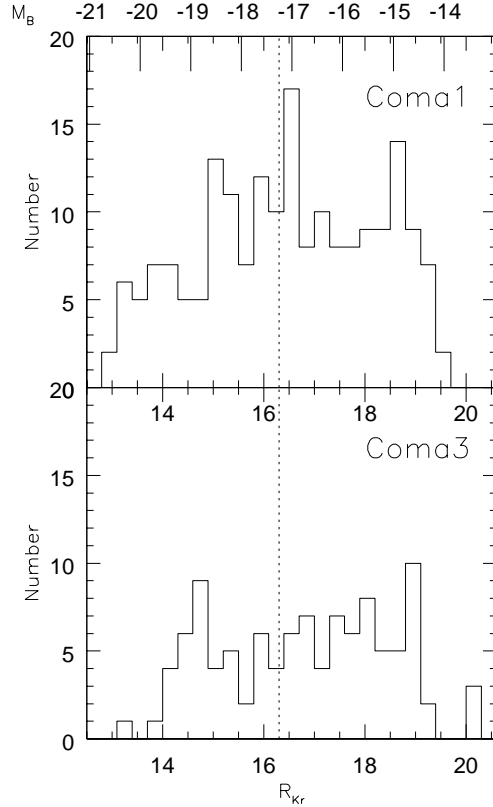


Fig. 1. The R band magnitude distributions of Coma1 and Coma3 galaxies that are cluster members. The corresponding absolute B magnitudes (at the top) have been found assuming a distance modulus to Coma of 35.16 ($\langle v \rangle = 7000 \text{ km s}^{-1}$, $H_0 = 65 \text{ km s}^{-1} \text{ Mpc}^{-1}$) and $B-R=1.6$. The dotted vertical line represents the adopted division between dwarfs and giants.

2.1. Lick indices

The Lick/IDS system (Burstein et al. 1984, Worthey et al. 1994, Trager et al. 1998) is the spectral index system that is most widely used to investigate the abundances and star formation histories of galaxies without current star formation. It is a convenient method to study practically all the main optical absorption lines in spectra of even modest resolution and it has the advantage that great theoretical effort has been devoted to interpret the results (see §3). The definitions of the Lick indices are shown in Table 1 and are taken from Trager et al. (1998) and Worthey & Ottaviani (1997). In this table we have flagged with an asterisk the numbers of those indices that will be used in this paper. All the indices listed in Table 1 have been measured in all our spectra, but here we will restrict our analysis only to galaxies with no detected emission lines. The presence of emission lines was assessed by inspecting each spectrum and interactively

searching for a line in emission at the wavelengths of the principal features ([OII]3727, H β , [OIII]4959,5007, H α , [NII]6548,6584), hence we cannot exclude that low-level emission (not apparent in a visual inspection) is present in some of our “non-emission-line” spectra. We note, however, that non-negligible emission (partially or totally filling-in, for example, the H β line) would be expected to show up as an emission line in H α or [OII], which are the lines most sensitive to even small amounts of photoionization; therefore, significant contamination of the Balmer indices in our non-emission line spectra seems unlikely.

In order to compare with the model predictions, it is first necessary to take into account: (a) the different spectral resolution of the WYFFOS spectra as compared to the Lick/IDS set-up; (b) the internal velocity dispersion of each galaxy; (c) any systematic offsets in the indices mainly due to the fact that the Lick stars were not flux calibrated. This was done as described in Appendix A. The final, fully-corrected indices of the Lick system were computed by a FORTRAN program that reads in the raw measurements (obtained after applying the correction for spectral resolution described in point a) of Appendix A), computes and applies the velocity dispersion corrections and finally applies the systematic offsets (point c) of Appendix A).

To determine the random errors in our Lick indices, we followed the approach of González (1993), as explained and reproduced in Cardiel et al. (1998, C98). González has derived analytical formulae to evaluate the random index errors, taking into account the data, the statistical propagation of errors, and the variance in each pixel. Cardiel et al. show that, for most situations, the formulae of González agree very well with numerical simulations. We used the *raw* (ie. non flux-calibrated) spectra, de-redshifted to zero velocity, and accounted for both CCD gain and read-noise to calculate the total variance per pixel (eqn. 9 of C98). The errors in each of the atomic and molecular indices were then calculated using eqns. 5-7,11,12,13-18 of C98. Negative counts (representing poor sky subtraction) were ignored if they constituted less than half the pixels in a given bandpass (index or continuum); if more than half of the pixels in a given bandpass were negative, then the absolute value of the counts was used.

The correctness of the calibration of our indices onto the Lick/IDS system has been verified with a number of tests as described in Appendix B: from them, we conclude that our index calibration onto the Lick system has been successful and that – within the limitations and drawbacks intrinsic to the data and model uncertainties – we can determine ages and metallicities by comparing the galaxy measurements and the model predictions.

3. Models

Many authors have used stellar population models to compute Lick line indices for stellar populations of different ages and metallicities (Worthey 1994, Weiss, Peletier & Matteucci 1995, Buzzoni 1995, Vazdekis et al. 1996, Bressan, Chiosi & Tantalo 1996, Maraston 1998, Tantalo, Chiosi & Bressan 1998, Maraston, Greggio & Thomas 1999). The models adopted in this paper are those of Worthey (1994) in the new WEB version³ that is based upon the Padova isochrone library (Bertelli et al. 1994). The Padova-based models were preferred to the Yale version for two reasons. First, the Yale version of the model did not cover the low-metallicity, young corner ([Fe/H]<-0.225, age < 8 Gyr) which could be

³http://astro.sau.edu/~worthey/dial/dial_a_pad.html

TABLE 1
INDEX DEFINITIONS

N_i	Name	Index Bandpass	Blue Bandpass	Red bandpass	Units
01	CN ₁	4142.125 – 4177.125	4080.125-4117.625	4244.125-4284.125	mag
02	CN ₂	4142.125 – 4177.125	4083.875-4096.375	4244.125-4284.125	mag
03	Ca4227	4222.250 – 4234.750	4211.000-4219.750	4241.000-4251.000	Å
04	G4300	4281.375 – 4316.375	4266.375-4282.625	4318.875-4335.125	Å
05	Fe4383	4369.125 – 4420.375	4359.125-4370.375	4442.875-4455.375	Å
06	Ca4455	4452.125 – 4474.625	4445.875-4454.625	4477.125-4492.125	Å
07	Fe4531	4514.250 – 4559.250	4504.250-4514.250	4560.500-4579.250	Å
08*	C ₂ 4668	4634.000 – 4720.250	4611.500-4630.250	4742.750-4756.500	Å
09*	H _{β}	4847.875 – 4876.625	4827.875-4847.875	4876.625-4891.625	Å
10	Fe5015	4977.750 – 5054.000	4946.500-4977.750	5054.000-5065.250	Å
11	Mg ₁	5069.125 – 5134.125	4895.125-4957.625	5301.125-5366.125	mag
12*	Mg ₂	5154.125 – 5196.625	4895.125-4957.625	5301.125-5366.125	mag
13	Mgb	5160.125 – 5192.625	5142.625-5161.375	5191.375-5206.375	Å
14	Fe5270	5245.650 – 5285.650	5233.150-5248.150	5285.650-5318.150	Å
15	Fe5335	5312.125 – 5352.125	5304.625-5315.875	5353.375-5363.375	Å
16	Fe5406	5387.500 – 5415.000	5376.250-5387.500	5415.000-5425.000	Å
17	Fe5709	5696.625 – 5720.375	5672.875-5696.625	5722.875-5736.625	Å
18	Fe5782	5776.625 – 5796.625	5765.375-5775.375	5797.875-5811.625	Å
19	Na D	5876.875 – 5909.375	5860.625-5875.625	5922.125-5948.125	Å
20	TiO ₁	5936.625 – 5994.125	5816.625-5849.125	6038.625-6103.625	mag
21	TiO ₂	6189.625 – 6272.125	6066.625-6141.625	6372.625-6415.125	mag
22	H δ _A	4083.500 – 4122.250	4041.600-4079.750	4128.500-4161.000	Å
23	H γ _A	4319.750 – 4363.500	4283.500-4319.750	4367.250-4419.750	Å
24*	H δ _F	4091.000 – 4112.250	4057.250-4088.500	4114.750-4137.250	Å
25*	H γ _F	4331.250 – 4352.250	4283.500-4319.750	4354.750-4384.750	Å
26*	< Fe >	(Fe5270+Fe5335)/2			Å
27	[MgFe]	$\sqrt{\text{Mgb} \cdot \text{< Fe >}}$			Å

relevant in this study⁴ while the Padova version has ages in the range 0.4-19.9 Gyr and $[\text{Fe}/\text{H}]$ between -1.7 and +0.4. Second, the Padova isochrones include the existence of blue horizontal branches (HB) in old populations of low metallicities. A blue HB produces moderate Balmer line strengths, hence an accurate treatment of the HB is needed for a correct interpretation of these lines (Poggianti & Barbaro 1997, Lee, Yoon & Lee 2000, Maraston & Thomas 2000). The Padova version reproduces well the increase in Balmer indices with decreasing metallicity observed in old populations (e.g. Galactic globular clusters).⁵ We have used Worthey’s WEB model interpolation engine to produce grids of indices of Single Stellar Populations with a standard Salpeter IMF ($x=2.35$, $M = 0.6 - 120M_{\odot}$) for ages=0.4,0.5,0.7,0.8,1.0,1.5,2.0,3.0,4.0,5.0,6.0,7.0,8.0,9.0,10.0,11.0,12.0,13.0,14.0,15.0,16.0,17.0,18.0,19.0,19.99 Gyr and $[\text{Fe}/\text{H}]=-1.7,-1.5,-1.3,-1.0,-0.7,-0.5,-0.25,0.0,0.25,0.39$. Another complete set of predicted Lick indices is given by Vazdekis et al. (1996) for ages between 1 and 17.4 Gyr and six metallicities between $[\text{Fe}/\text{H}]=-1.7$ and +0.4. This set is based upon the Padova isochrones as well, and therefore has the same stellar evolutionary background as the models used in this paper. Comparing the synthetic grids of the indices employed in §4.2 for the same IMF, we found a general agreement between the Worthey and Vazdekis models. The only systematic difference was that Vazdekis’s models reach slightly lower values of $\text{H}\beta$ ($\sim 0.2 \text{ \AA}$ lower) at old ages (> 14 Gyr) and slightly higher values (0.01 mag) of Mg_2 at low metallicity (≤ -0.7), producing at most a ~ 0.1 difference in Z and an age difference smaller than the uncertainty at old ages. Both sets of models lead to the conclusions presented below, and we decided to use Worthey’s models because they allowed us to produce a model grid as fine as desired, in the range 0.4 to 20 Gyr (but see also Vazdekis’s WEB page for an update of his models).

It is generally assumed that the calibrating stars used to derive the Lick/IDS fitting functions adopted in the models have solar abundance ratios; more likely, there is a variation of abundance ratio built into the models, for example the calibrating globular cluster (low metallicity) stars have $[\text{Mg}/\text{Fe}]$ ratios above solar (Worthey 1998). Under the (likely correct) assumption that *around solar metallicity* the model ratios are indeed solar, it has been found that luminous ellipticals have non-solar abundance ratios and that the $[\text{Mg}/\text{Fe}]$ ratio increases with the luminosity (Peletier 1989, Worthey et al. 1992, Vazdekis et al. 1997, Worthey 1998 and references therein, Trager et al. 2000a and 2000b, Kuntschner et al. 2001). Originally referred to as a magnesium enhancement, this effect is now recognized to be more precisely an iron depression (Vazdekis et al. 1997, Trager et al. 2000a).

In this paper we do not attempt to vary the $[\text{Mg}/\text{Fe}]$ ratio of the models because (a) the variations of the ratio *intrinsic* to the models are not well understood over the metallicity range of interest here, and (b) our sample does not comprise extremely luminous galaxies ($M_B < -21$), and consists mostly of low luminosity objects which are believed to be consistent with solar abundance $[\text{Mg}/\text{Fe}]$ ratios (e.g. Gorgas et al. 1997). However, we caution that solar abundance ratios in low luminosity galaxies are usually deduced from the agreement with models which probably *do not* have solar ratios at low metallicities, as explained above. In the following, we will employ both iron and magnesium indices and compare the results obtained.

⁴In fact, this region of the parameter space turned out to be populated by a significant fraction of our dwarf galaxies, see later.

⁵As an example, the $\text{H}\beta$ index of the models used in this paper is 2.6 for $[\text{Fe}/\text{H}]=-1.7$, 2.5 at $[\text{Fe}/\text{H}]=-1.5$ and 2.4 at $[\text{Fe}/\text{H}]=-1.3$ (compare with Fig. 1 in Maraston & Thomas 2000).

4. Results

4.1. Index results

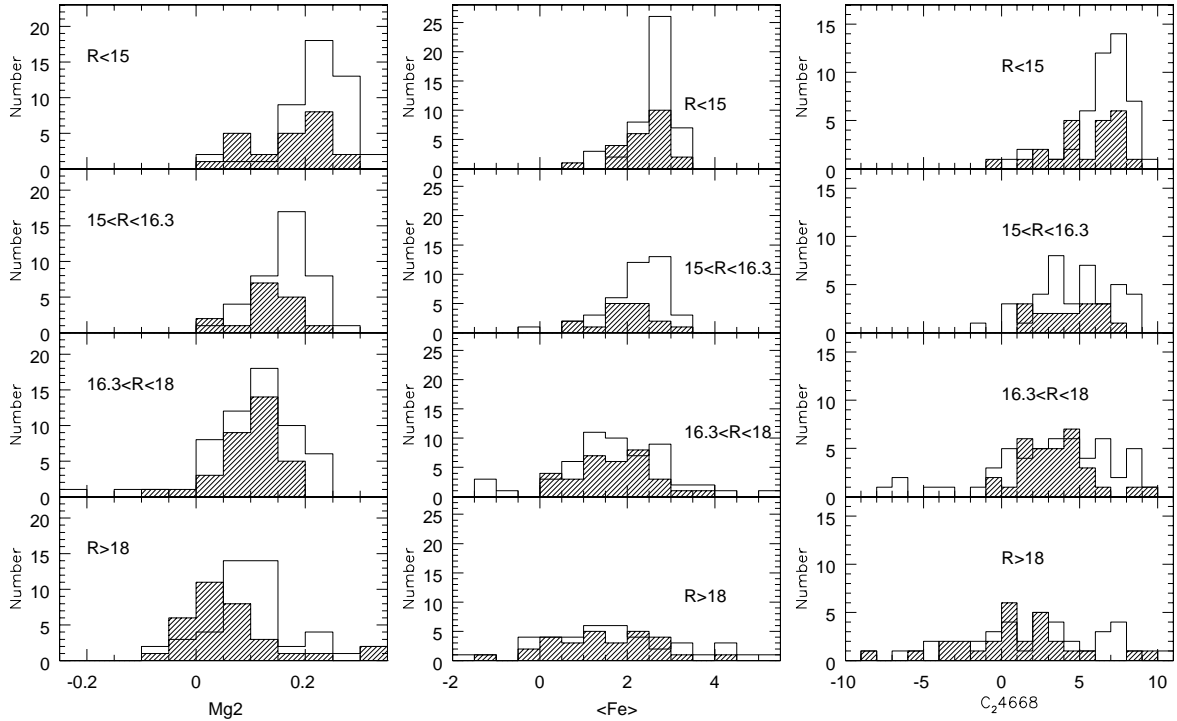
The distributions of the most relevant indices are shown in Fig. 2 for four magnitude bins and for Coma1 and Coma3 galaxies separately (empty and shaded histogram respectively). Three main results appear evident:

a) For both fields, the mean value of the metallicity-sensitive indices (Mg_2 , $\langle Fe \rangle$, C_{24668}) *increases* for brighter galaxies. Similarly, the mean value of the age-sensitive (Balmer) indices *decreases* with galaxy luminosity.

b) Within a given magnitude bin, in the Coma1 region there is generally a higher proportion of galaxies with higher metallicity-indices and lower age-indices than in Coma3.

c) The width of the distributions increases towards fainter galaxies.

In the following we will mostly focus on the trends of the spectral indices with magnitude for the whole sample (Coma1+Coma3), pointing out the differences between Coma1 and Coma3 only when luminosity and environmental effects need to be disentangled. The spatial dependence of the galaxy properties will be presented in a future paper of the series.



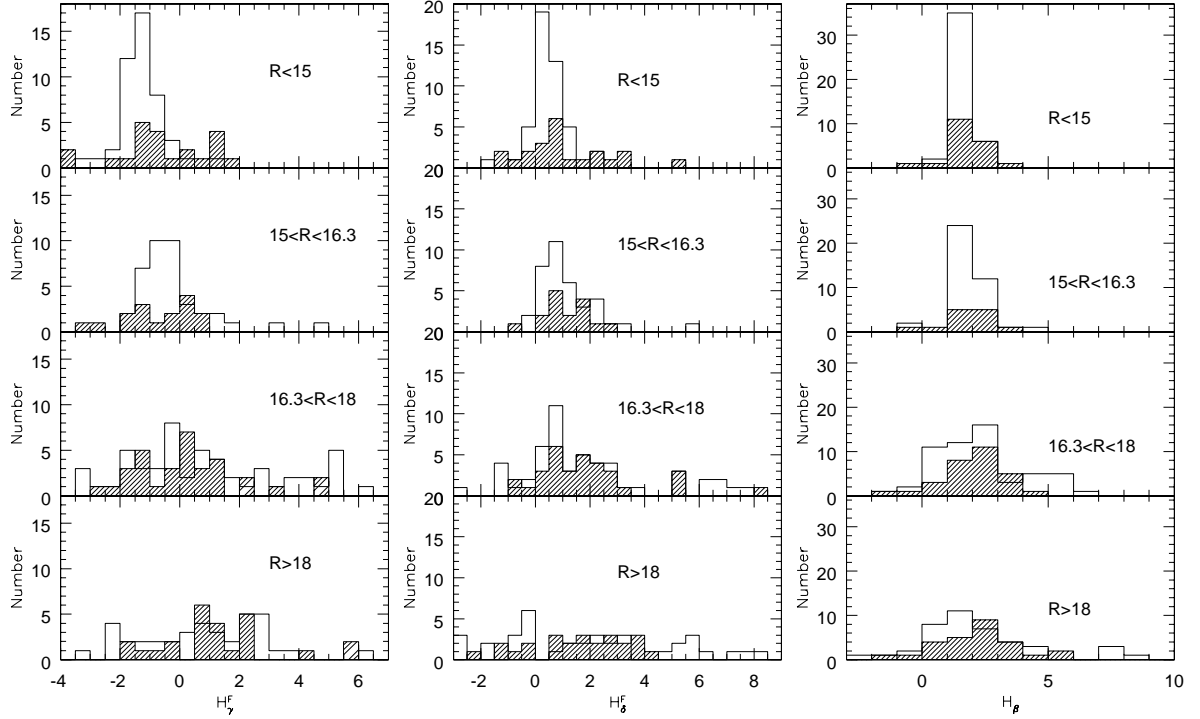


Fig. 2. Index distributions of Coma1 (empty histogram) and Coma3 (shaded histogram) galaxies for four magnitude bins. Emission line galaxies have been excluded.

The trends of the indices with galaxy luminosity are shown clearly in Fig. 3, where it can be seen that there is a positive correlation between the age-sensitive indices and R magnitude, and an anticorrelation between the metallicity-sensitive indices and R magnitude.⁶ It is remarkable that these relations hold over the whole magnitude range explored in this study (6.5 mag) down to $M_B \sim -14$. The scatter around these relations progressively increases for fainter galaxies and a group of distinguished outliers – mainly dwarfs – can be identified in most of these plots. Note that the incidence of outliers, especially in the Balmer-indices plots, is not symmetric around the mean relation, and there are many more points lying *above* the relation than below. The remainder of this section deals with the interpretation of the mean observed relations, the origin of the scatter and the characteristics of the outliers⁷.

We find that correlations similar to those of Fig. 3 exist also between the indices and the R -band effective surface brightness μ . This is not surprising given the correlation between the R magnitude and the effective surface brightness observed in this sample (Mobasher et al. 2001, Paper II). The slope B and the intercept A of the linear fits to the data are given in Table 2 for the relations of six indices with the R magnitude and with μ .

⁶Similar relations are found for other metallicity-sensitive and age-sensitive indices but not shown.

⁷We note that the majority of the outliers in the right-hand plots are not the same objects that stand out as outliers in the left-hand plots. This will become clearer examining the index-index diagrams in the next section. As an example, most of the $H\beta$ -strong galaxies with $H\beta > 4$ have $Mg2 < 0.2$.

Since there is no such a thing as a “pure” index that depends only on age or only on metallicity, each of the correlations shown in Fig. 3 implies either that the fainter galaxies are younger, or that they are less metal rich, or both. In order to separate these effects it is necessary to compare the positions of the galaxies in index-index plots with the results of our models.

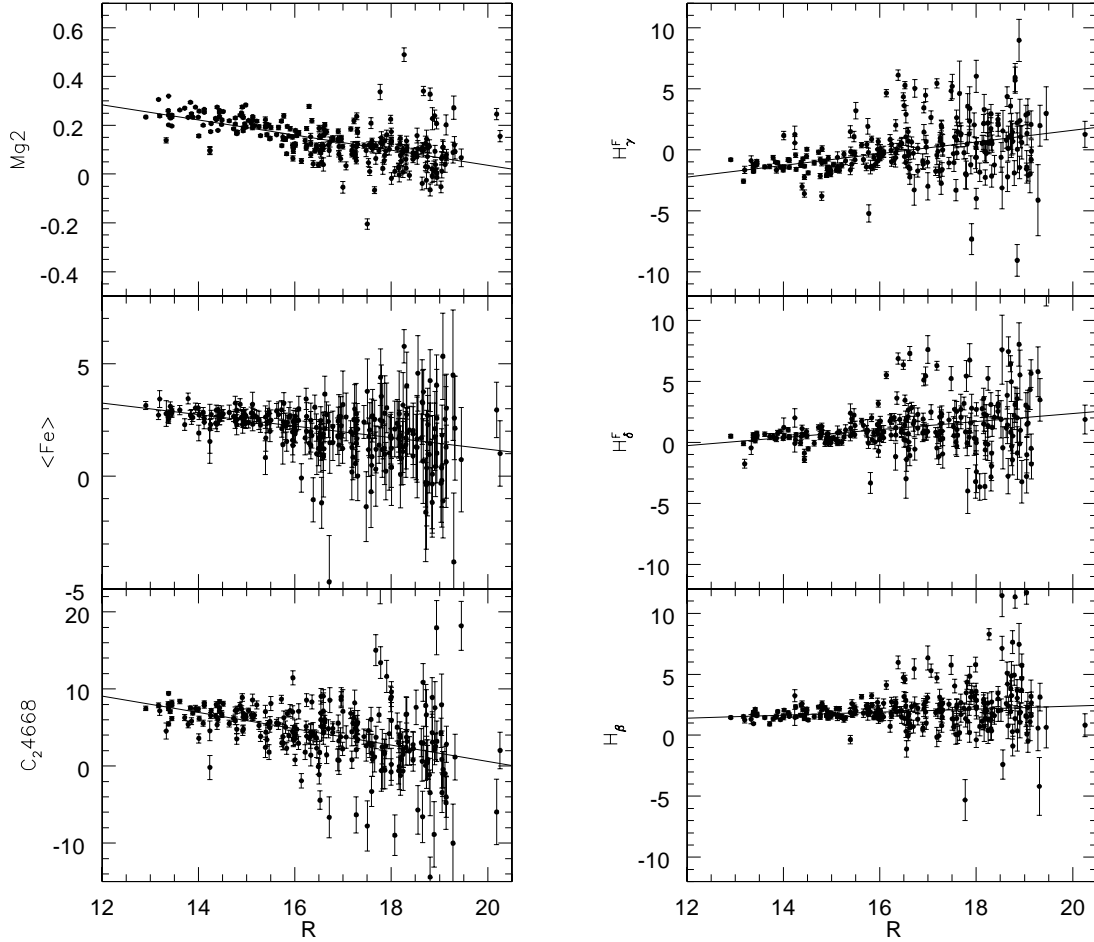


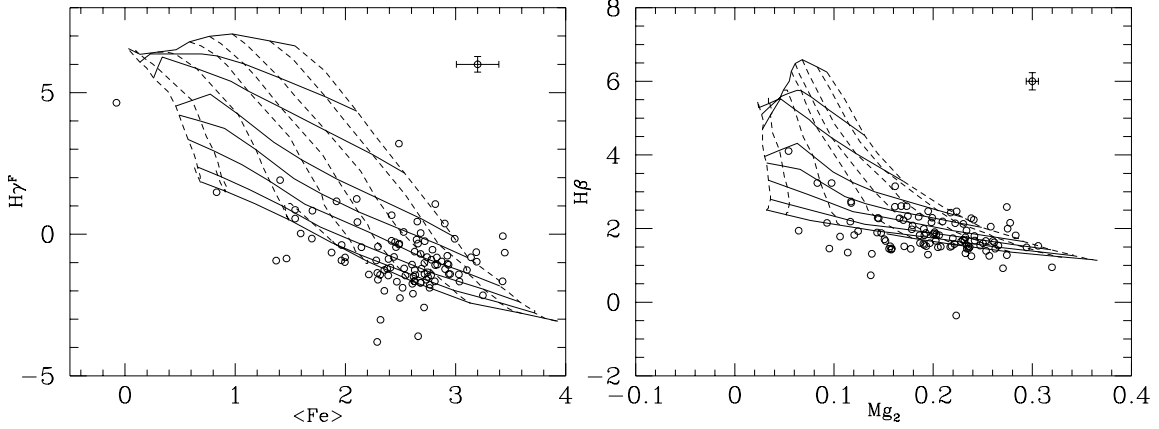
Fig. 3. The relations between R magnitude and the metallicity-sensitive indices (left), and the age-sensitive indices (right). Emission-line galaxies have been omitted from this figure. Both Coma1 and Coma3 galaxies are included. The straight line in each panel is a robust linear fit to the data found by means of an M-estimate that minimizes the absolute deviation; the slope B and the intercept A of these fits are given in Table 2.

4.2. Index-index diagrams

In this section we wish to investigate whether the trends of the indices with galaxy magnitude presented in §4.1 are due to metallicity, age, or both. To discriminate between these effects it is necessary to analyse simultaneously an age-sensitive index and a metallicity-sensitive index. Comparing them with a

two-dimensional theoretical grid of single stellar populations (single burst and single metallicity at a given age) yields an estimate of the *luminosity-weighted* age and metallicity of the galaxy.

Figure 4 shows the index-index plots of the dwarf (filled circles) and giant (empty circles) samples. Here we present the two most age-sensitive indices according to Worthey & Ottaviani (1997) ($H\beta$ and $H\gamma_F$) versus two indices which are mostly sensitive to metallicity (Mg_2 and $\langle Fe \rangle$)⁸. A subset of the model grid is shown in more detail in Fig. 5.



⁸Although the C_{24668} index shows the strongest sensitivity to metallicity (Worthey & Ottaviani 1997, Worthey 1998), we preferred to use the other metallicity indicators because the reliability of C_{24668} has been questioned (Jones, Smail & Couch 2000) and it is unclear what chemical species drives its enhancement with respect to iron in the most luminous galaxies (Kuntschner 2000).

TABLE 2
PARAMETERS OF THE FIT $Y = A + B \times R$ (or μ)

Y	A_R	B_R	A_μ	B_μ
Mg_2	0.656	-0.031	0.947	-0.038
$\langle Fe \rangle$	6.299	-0.255	9.228	-0.343
C_{24668}	21.8	-1.06	31.56	-1.302
$H\gamma_F$	-7.994	0.479	-15.70	0.753
$H\delta_F$	-4.238	0.331	-8.705	0.478
$H\beta$	-0.139	0.127	-1.79	0.180
$Z(Hb)$	3.006	-0.220		
$Z(Hg)$	1.944	-0.144		

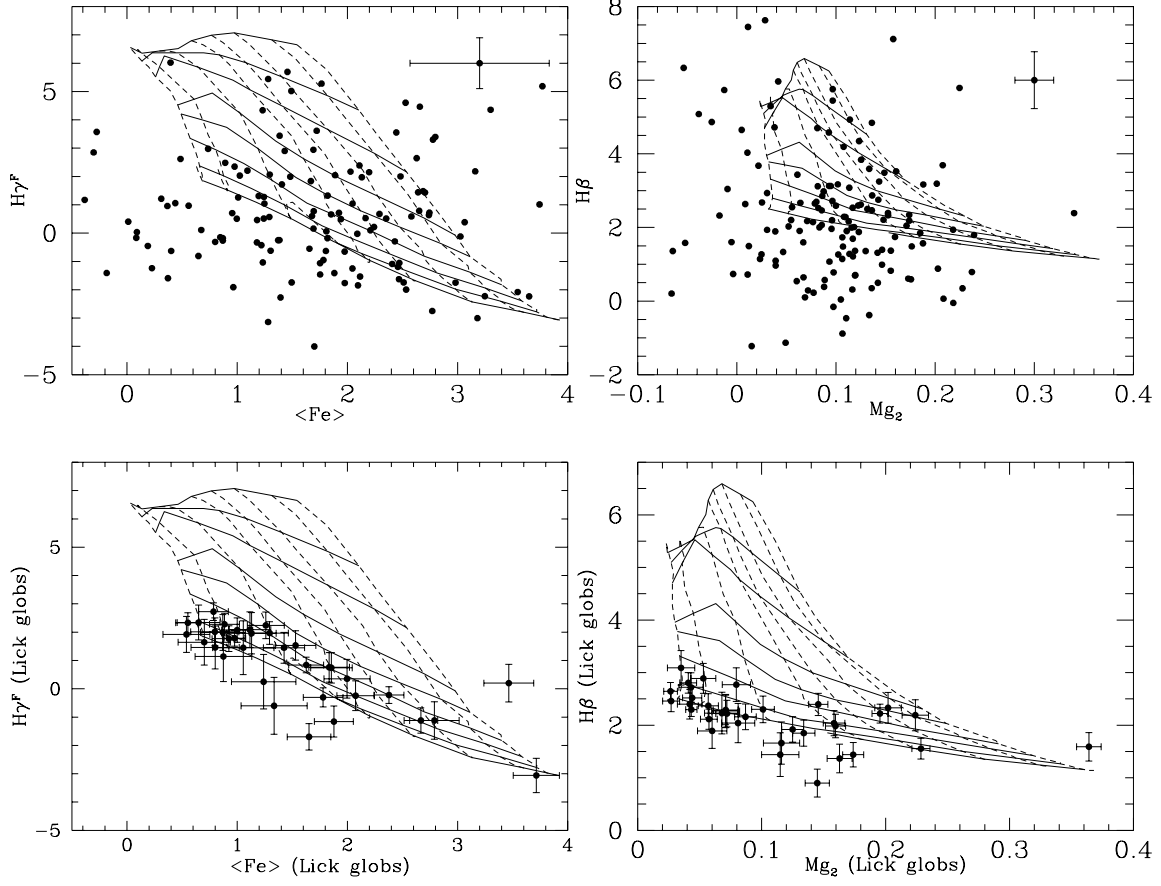


Fig. 4. The two best age-sensitive indices ($H\gamma_F$ and $H\beta$) are plotted against two metallicity-sensitive indices ($\langle Fe \rangle$ and Mg_2). Top and middle panels: giant (empty symbols) and dwarf (filled symbols) galaxies, respectively. For clarity, only the mean errorbars for dwarfs and giants are shown in the top right corner of the plot. Overplotted are some Padova models by Worthey (see §3) of single stellar populations (see Fig. 5). Bottom panels: results for Lick globular clusters, kindly provided by G. Worthey ahead of publication.

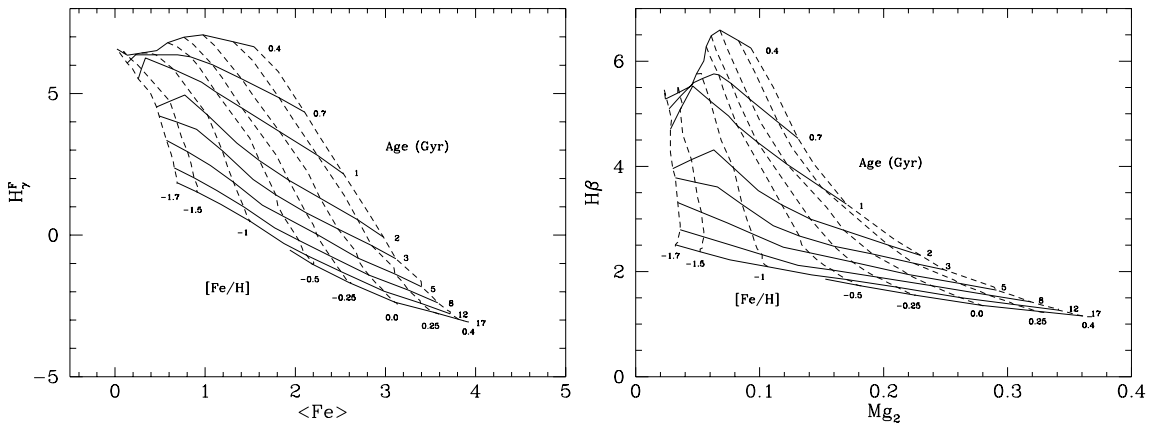


Fig. 5. Model grids as in Fig. 4. For clarity only a subset of the model set is displayed (§3). Note that the age resolution decreases with age and that the model grid is practically degenerate at ages greater than $\sim 9 - 10$ Gyr.

A first, visual inspection of these diagrams allows us to draw some qualitative conclusions and reveals that:

- 1) Most of the giant galaxies lie in the high-metallicity and old age corner of the model grid ($[\text{Fe}/\text{H}] > -0.25, t > 5$ Gyr).
- 2) Dwarf galaxies occupy a larger region than giants in the diagrams, covering the whole range of metallicity but mostly lying at $[\text{Fe}/\text{H}] < -0.25$. They have a broad range in ages, from very old to young (< 1 Gyr), but the majority of them reside in a region where the models are older than 3 Gyr. Their metallicity-index range overlaps with that of the Lick globular clusters (kindly provided by G. Worthey ahead of publication, bottom panels in Fig. 4), while their age-index range extends to ages much lower than those of the globular clusters.
- 3) The errorbars on the indices of the giant galaxies are quite small (e.g. the mean $\sigma_{\text{H}\beta} = 0.16$ and $\sigma_{\text{Mg}_2} = 0.004$ for $R < 15$, mean $\sigma_{\text{H}\beta} = 0.22$ and $\sigma_{\text{Mg}_2} = 0.006$ for $R < 16.3$). For comparison, the mean errors in the Lick/IDS sample of galaxies are $\sigma_{\text{H}\beta} = 0.31$ and $\sigma_{\text{Mg}_2} = 0.009$. On the contrary, the index errors for fainter galaxies in our sample are large, with a mean $\sigma_{\text{H}\beta} = 0.68$ and $\sigma_{\text{Mg}_2} = 0.020$ for the whole dwarf subsample ($R > 16.3$). This reflects the variation of mean signal-to-noise with magnitude. The mean S/N measured between 4800 and 5200 Å is 15.5, 13.8, 8.6 and 7.8 for $R < 15$, $15 < R < 16.3$, $16.3 < R < 18$ and $R > 18$, respectively. Large errors are a critical issue for the dwarf galaxies, and allow us to obtain only broad general conclusions regarding their ages and metallicities, as discussed in the next sections.
- 4) Quite a large number of datapoints (mostly dwarfs) lie outside of the model grid. As explained in §3, the grid extends over the ranges $[\text{Fe}/\text{H}] = -1.7/0.4$ and $t = 0.4/20$ Gyr. The most notable group of outliers is located *below* the grid, at very low Balmer indices. While some of these outliers overlap with the grid if their errorbars are taken into account, many of them display Balmer indices which are far too low compared with those of any model.

The same problem has been observed in the spectra of a number of globular clusters (Rose 1994, Jones 1996, Cohen, Blakeslee & Ryzhov 1998, Vazdekis & Arimoto 1999) and it is also apparent in the bottom panels of Fig. 4 showing the results of the Lick globular clusters. The best-studied case is the metal-rich globular cluster 47 Tuc, whose high-resolution, high-signal-to-noise spectra yield very low Balmer indices, implying an embarrassing spectroscopic age > 20 Gyr (Gibson et al. 1999; Vazdekis et al. 2001) which is at odds with the age derived from the resolved color-magnitude diagram (9-14 Gyr). A number of early-type galaxies with $H\beta$ indices below the model grid have also been found by Kuntschner et al. (2001). Nebular emission appears unlikely to be the source of the discrepancy (Gibson et al. 1999; Vazdekis et al. 2001, Kuntschner et al. 2001); in our case, if emission were the main cause of the low Balmer lines we would expect this phenomenon to be much more prominent in $H\beta$ (right panel in Fig. 4) than in $H\gamma$ (left panel in Fig. 4) and this is not the case. It has been suggested that the reason might be a problem in the zero point of the models which probably fail to reach sufficiently low Balmer line strengths at old ages due to the fact that the main sequence turnoff (TO) is cooler than current models assume (Vazdekis et al. 2001; also Alexandre Vazdekis (1999) and Scott Trager (2000), private communications). In fact, there are suggestions from recent developments of stellar evolution theory that improving the input physics of the models (i.e. including the effects of diffusion and the Coulomb correction to the equation of state) produces a decrease of the turnoff temperature (Lee, Yoon & Lee 2000 and references therein, Vazdekis et al. 2001). If this is the cause of the mismatch between the models and the low Balmer indices observed and if the metallicity estimate is sufficiently unaffected by the TO temperature as argued by Vazdekis et al. (2001), then the objects lying below the model grids in Fig. 4 are old stellar systems (luminosity-weighted age > 9 Gyr) whose approximate metallicity can be inferred from their metallicity-index. Adopting this as our working hypothesis, we derived relative ages and metallicities as explained below.

4.3. Ages and metallicities

The age-index versus Z-index plots of Fig. 4 were used to derive the values of the luminosity-weighted stellar ages and metallicities. Given a chosen pair of indices, we computed the age and abundance of each datapoint lying within the model grid interpolating from the closest model points. In the case of the low-Balmer points below the grid, the abundance was estimated extrapolating the iso-Z model lines (dashed lines in Fig. 4) and an old age, arbitrarily recorded as 30 Gyr to keep track of these objects, was assigned. Similarly, the age of the few points lying to the right(left) of the model grid was estimated extrapolating the iso-age model lines and an arbitrarily high(low) metallicity was recorded ($[Fe/H]=+3(-3)$). Errors were found by perturbing the index values with their errorbar and recomputing the age and Z.⁹

The luminosity-weighted metallicities derived from the two pairs of indices are shown as a function of galaxy luminosity in Fig. 6. In both cases the mean metallicity increases towards brighter magnitudes. A straight line fit to the $Z(H\beta)$ estimate (based on the $H\beta/Mg_2$ model grid) yields somewhat lower metallicity

⁹We remind the reader that in this paper the metallicity “Z” is $Z = [M/H] = \log(M/H) - \log(M/H)_\odot$ where M represents the “metal” content. In the case of solar abundance ratios, $[Fe/H]=[Mg/H]=[any\ other\ heavy\ element/H]=[Z/H]$ where Z indicates the sum of all elements heavier than helium. Since variation in abundance ratios might be present within our sample, it should be kept in mind that Z indicates the total metallic content as determined either by the magnesium or the iron indices.

values at faint magnitudes than the $H\gamma_F$ -based estimate, possibly due to varying abundance ratios. The parameters of the best fit Z-R relations are given in Table 2.

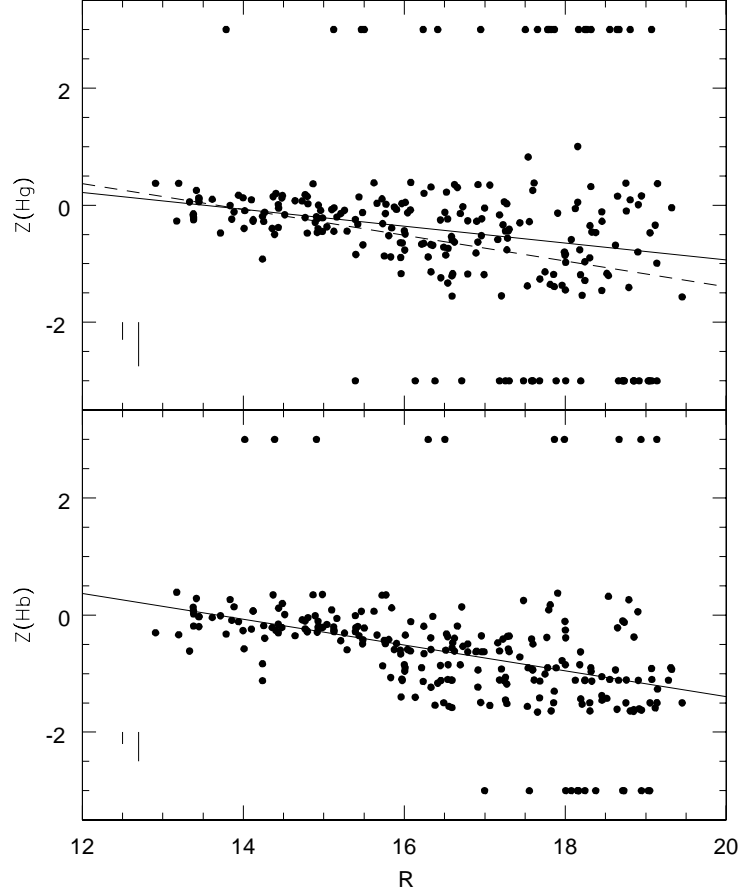


Fig. 6. Metallicities derived from the comparison with the model grids $H\gamma_F/\langle Fe \rangle$ (top panel) and $H\beta/Mg_2$ (bottom panel) are plotted against the R band magnitude. Best fit relations are shown as solid lines. The best-fit line of the bottom panel ($Z(Hb)$ vs. R) is shown as the long dashed line in the top panel for comparison. The typical errorbars for giants and dwarfs are found in the left bottom corner of each panel. Note that, while the mean $Z(Hg)$ shows a steady decline with R , the mean $Z(Hb)$ - R relation appears to be almost flat for giants and drops to lower values for the dwarfs, with a break at around $R=16$. It is unclear whether this effect is real, or is an artifact due to the combination of the errors and the shape of the model grid.

Hence, a correlation between metallicity and luminosity exists for galaxies in our sample. The spread in metallicity is much larger at faint magnitudes, as clearly shown by the Z distributions presented in Fig. 8. In this figure the arrows represent the mean metallicity in each magnitude bin of Coma1 (solid arrow) and Coma3 (dotted arrow) galaxies. It is beyond the scope of this paper to discuss the variation of the galactic properties as a function of the position in the cluster, but we note here that Coma1 galaxies tend to be on average more metal-rich than Coma3 galaxies in any given magnitude interval. This finding could be consistent with the result of Secker (1996), who detected a color gradient in the projected radial distribution of Coma dwarf ellipticals which he interpreted as an increase in metallicity closer to the cluster centre.

In contrast to metallicity, age does not correlate with R in a simple way (Fig. 7). However, we are going to show that there are systematic trends in the proportion of galaxies of different ages with luminosity. First of all, in Fig. 7 it is possible to notice two voids in the left bottom corner and in the right top corner of the diagram, corresponding to a lack of young bright galaxies and of old faint galaxies. The top right void disappears if one takes into account the numerous points lying at age=30 Gyr. The corresponding age distributions are presented in Fig. 8 for Coma1 and Coma3 galaxies in each magnitude bin. The mean ages found from $H\gamma_F$ are typically 1 Gyr younger than the corresponding mean $H\beta$ ages of the same magnitude bin. In Coma1, the mean age slightly decreases towards fainter galaxies, ranging from 9.3 ($R < 15$) to 7.6 Gyr ($R > 18$) for $H\gamma_F$ and from 10.0 to 8.4 Gyr for $H\beta$. There is no obvious trend in the mean age of Coma3 galaxies for different magnitude bins, possibly due to small number statistics, and we note that bright galaxies in Coma3 are on average younger than in Coma1.

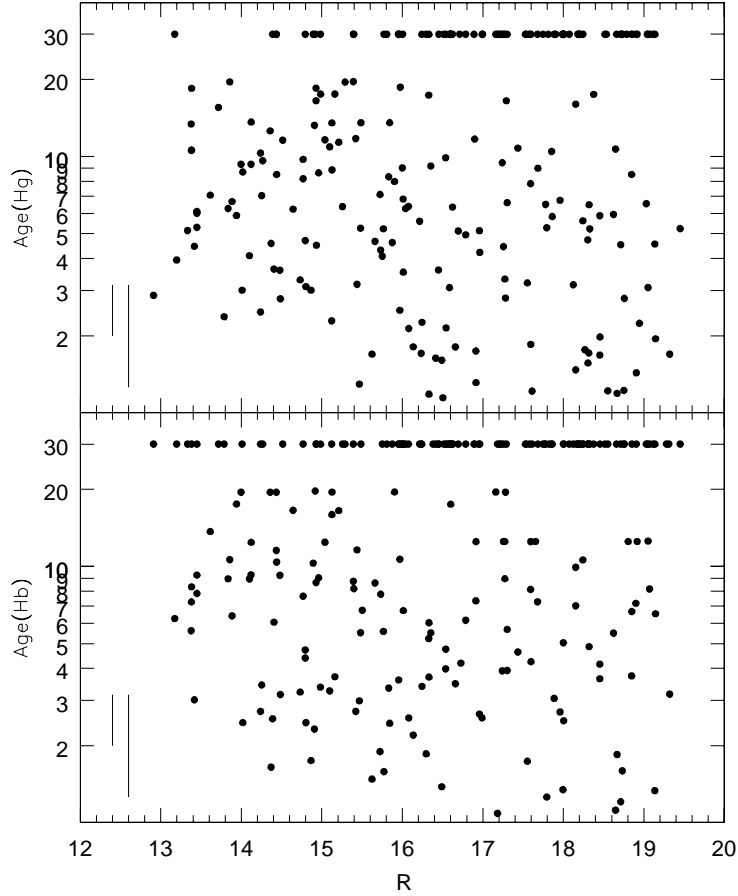


Fig. 7. Ages derived from the model grids $H\gamma - F / \langle Fe \rangle$ (top panel) and $H\beta / Mg_2$ (bottom panel) plotted against R magnitude. The typical errorbars of dwarfs and giants are shown in the left bottom corner. The *length* of the errors is approximately constant throughout the diagram and corresponds to an uncertainty of 1-2 Gyr at ages < 4 and to several Gyrs at older ages. This is because the age resolution decreases roughly logarithmically for older populations.

Since the errorbars of the indices of faint galaxies are too large to look for subtle differences (such

as for example 1 Gyr at old ages or 0.1 dex in Z), we have grouped all galaxies into three broad age and metallicity classes: old (age > 9 Gyr), intermediate ($3 < \text{age} < 9$ Gyr), young (age < 3 Gyr) and metal-rich ($Z > -0.15$), intermediate $-1 < Z < -0.15$, and metal-poor $Z < -1$. The ranges chosen for these classes are broader than the uncertainty of even the faintest galaxies, thus it is safe to draw conclusions on the basis of this classification. Repeated spectra of 9 dwarf galaxies confirm the robustness of this broad division in classes and show that this is actually a conservative choice.

The proportions of young, intermediate-age and old galaxies among Coma1 galaxies of each magnitude bin are shown in Fig. 9. Interestingly, the fraction of old galaxies is approximately constant within the errors regardless of the magnitude, while the fraction of young galaxies increases towards *fainter* magnitudes and the fraction of intermediate-age galaxies increases towards *brighter* magnitudes.¹⁰ The absolute values of these fractions depend on which index-index diagram is considered (compare left and right panels in Fig. 9), but the trends are the same in both cases. This is a striking result, if one considers that a look-back time of 3 Gyr corresponds to $z \sim 0.35$ ($H_0 = 65 \text{ km s}^{-1} \text{ Mpc}^{-1}$, $q_0 = 0.05$), 5 Gyr to $z \sim 0.65$ and 9 Gyr to $z \sim 2$. If the luminosity-weighted age can be considered to be approximately representative of the epoch of the last episode of significant star formation¹¹ (Trager et al. 2000b), taking Fig. 9 at face value implies that among the galaxies without active star formation at $z=0$ in the central region of Coma:

a) about 50 to 60% of them did not have significant star formation activity since $z \sim 2$ (old galaxies). Remarkably, these figures are valid for both giants and dwarfs over 6 magnitudes, regardless of the luminosity. Conversely, this means that about 40-50% of the present-day non-active cluster population – at all magnitudes – *did* have significant star formation at redshifts below 2.

b) the fraction of (present-day) *luminous* galaxies that have had significant star formation in the intermediate-redshift regime between $z=2$ and $z=0.35$ (intermediate-age galaxies) was higher than the fraction of (present-day) *dwarfs* that were active at that epoch;

c) at low-redshift ($z < 0.35$), the star formation activity has involved a higher proportion of faint galaxies than bright ones.

These fractions are found simply considering the ages derived from the $H\beta - \text{Mg}_2$ diagram and ignoring the effects of the errors on the index measurements. The errors are relatively small and will not significantly affect the proportions of young, intermediate-age and old galaxies in the two brightest magnitude bins of Fig. 9 (giant galaxies, see §4.2), but they are large and can potentially have systematic effects on the fractions of dwarfs (faintest two bins in Fig. 9). To assess how relevant this can be, we have recomputed the fractions of dwarfs excluding from the “old” and “young” classes all those galaxies whose errorbars are large enough to possibly move them into a different age class. In this way, we derive a “minimum” fraction of “secure” old dwarfs $\sim 30\%$ and of “secure” young dwarfs $\sim 20\%$. Assuming the error estimates are realistic, these are lower limits for the proportions of old and young dwarfs. The fraction in the intermediate-age class is obviously the most uncertain one, and could represent as much as 45% of the dwarf population, in the most pessimistic case that *all* those galaxies with large errorbars classified as old and young would instead fall into the intermediate class. In conclusion, it is important to keep in mind that a realistic

¹⁰The trends might be similar for Coma3 galaxies but for them the Poissonian errorbars are too large to reach any firm conclusions.

¹¹In general, the luminosity-weighted age will be an upper limit to the time elapsed since the last star formation activity, because it is diluted by the light of all previous stellar populations.

uncertainty on the fractions for the two faintest bins presented in Fig. 9 is surely larger than the Poissonian errorbars shown. However, even taking the errors into account, two results appear to be solid: 1) the fraction of young dwarfs is higher ($\geq 20\%$) than the fraction of young giants, and 2) a significant fraction of the dwarfs (at least $\sim 1/3$ of them) have old luminosity weighted ages.

It is also worth recalling that the results discussed above refer to the central region of each galaxy (§2). If significant radial age gradients are present within a galaxy, these results cannot be considered representative of the whole star formation history. Since we cannot exclude that some SF activity occurred in the outer regions of the “old” galaxies, the values for young and intermediate-age galaxies of Fig. 9 are lower limits to the fractions of galaxies that experienced star formation at $z < 0.35$ and $0.35 < z < 2$.

These results provide some constraints for theories of galaxy evolution in clusters and especially dwarf galaxy evolution. They seem to point to a “down-sizing effect”, suggesting that the last star formation activity (possibly related to the epoch of accretion onto the cluster) occurs on average at lower redshifts for progressively fainter galaxies. This would imply that the “typical mass” of a star-forming galaxy in Coma decreases towards lower redshifts. Obviously, these findings will need to be compared with the accretion history of clusters predicted by hierarchical models. If these conclusions are representative of the evolutionary history of rich clusters in general, they represent a relatively precise local ($z=0$) assessment of the star formation history of the cluster galactic population to be compared with distant cluster studies. In a qualitative manner, these results agree with the photometric and spectroscopic studies of the Butcher-Oemler effect at intermediate redshifts which are mostly limited to luminous galaxies and find current or recently halted star formation activity in a large fraction of cluster galaxies at $z=0.3-0.6$ (Butcher & Oemler 1978, 1984; Dressler & Gunn 1982, 1983, 1992; Couch & Sharples 1987; Barger et al. 1996; Dressler et al. 1999; Poggianti et al. 1999). Totally passive (k-type) galaxies with no recent star formation (no SF at redshifts below 0.8 in the cosmology adopted here) were found to be typically 50% of the cluster population of 10 clusters at $z \sim 0.5$ (Poggianti et al. 1999).

Finally, it is extremely interesting that regardless of the variation in the epoch of the last SF episode in galaxies in this sample (Fig. 8), a general relation between the metallicity and the luminosity exists (Fig. 6), although with a significant scatter.¹² This could be suggesting that the relatively recent star formation we observe is due to secondary episodes that do not affect the chemical enrichment history of the galaxy sufficiently to demolish the luminosity-weighted Z versus luminosity relation which was likely established at earlier epochs.

¹²Another example of this are the dwarf galaxies of the Local Group, where galaxies with very diverse star formation histories follow the same global relations between absolute magnitude and mean metallicity (Caldwell 1999, Grebel & Guhathakurta 1999).

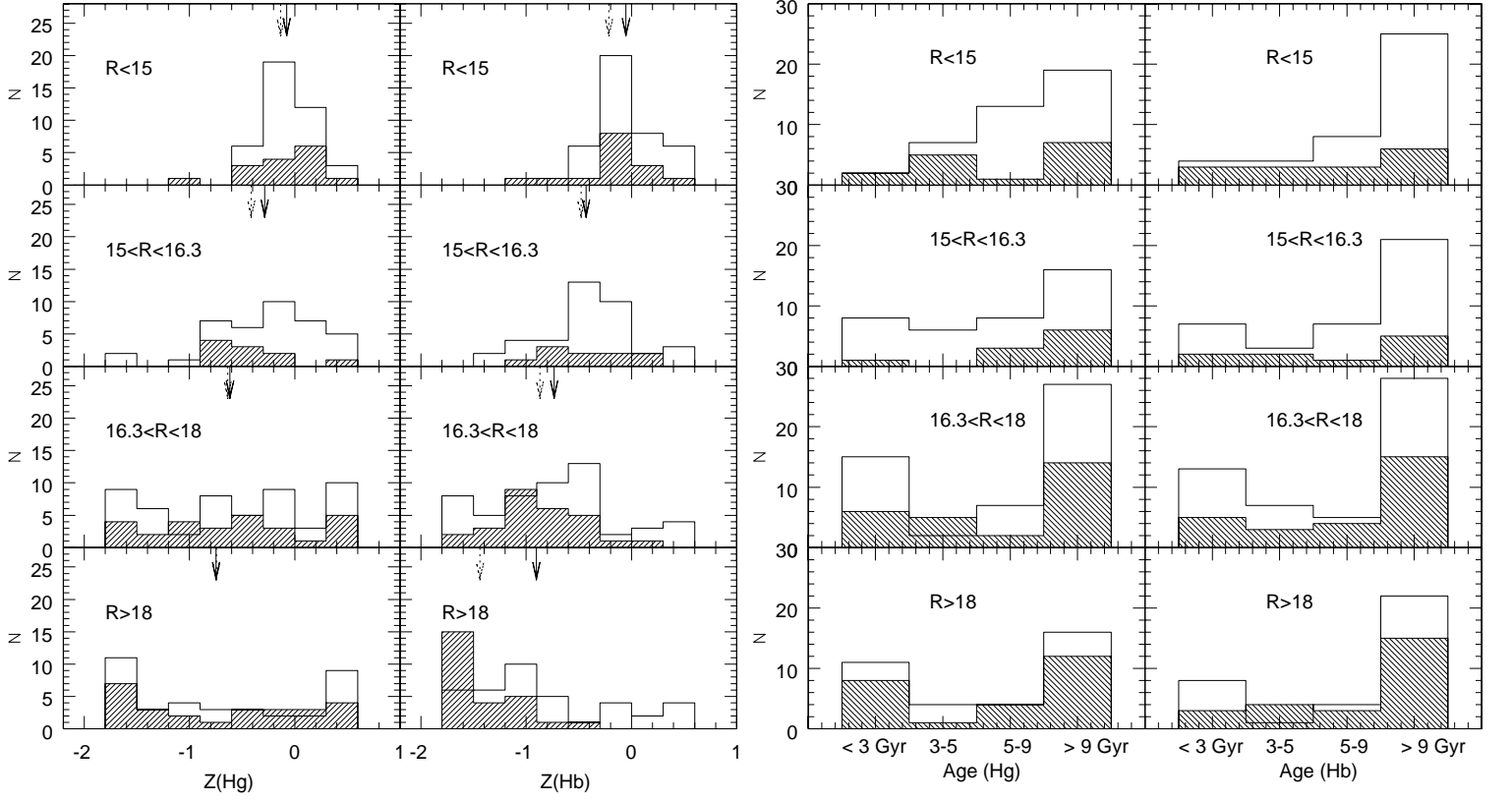


Fig. 8 Distributions of Z (left) and ages (right) for galaxies in the four magnitude bins. Empty and shaded histograms refer to Coma1 and Coma3 galaxies respectively. The arrows in the left panel indicate the mean value of Z in Coma1 (solid arrow) and Coma3 (dotted arrow) in each magnitude bin. In these diagrams the outliers ($Z=-3, +3$) have been assigned to $Z=0.5$ and $Z=-1.8$ respectively. The width of the bins has been chosen to be comparable to the uncertainties in age and Z for the faintest galaxies.

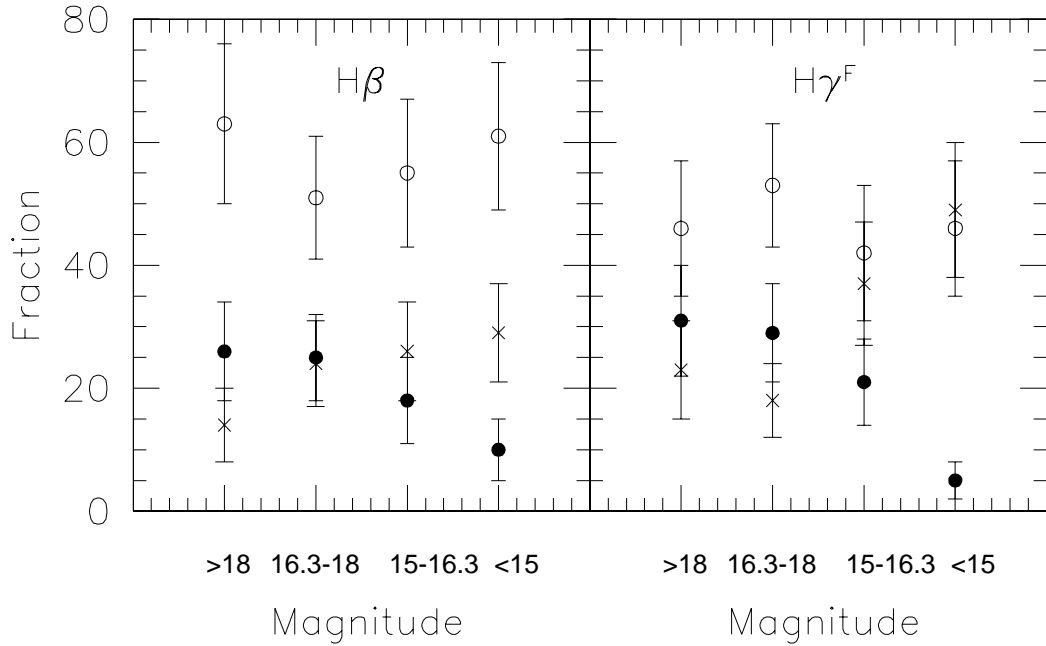


Fig. 9. Fraction of young (filled dots, age < 3 Gyr), intermediate-age (crosses, 3 to 9 Gyr) and old (empty dots, age > 9 Gyr) Coma1 galaxies within each magnitude bin as derived from the $H\beta/Mg_2$ diagram (left) and the $H\gamma_F/Fe$ diagram (right). The errorbars are Poissonian.

4.4. The composite nature of the faint galaxy population

We will now discuss the main properties of the faint galaxies in our sample, especially concentrating on the young ones. We stress that, given the large errors on individual measurements, conclusions for faint galaxies are reliable only in a statistical sense, not on a one-to-one basis. We have seen in §4.3 that at faint magnitudes ($R > 16.3$), more than half of the galaxies are old, $\sim 20\%$ have an intermediate age and

$\sim 25\%$ are young. We remind the reader once again that terms such as “old” and “young” refer to the luminosity-weighted integrated age and that these proportions are found having assumed that galaxies with very low Balmer indices (those lying below the model grid in Fig. 4) are indeed old. If the $H\beta$ index in some of these galaxies is actually contaminated by emission, then these are “young” galaxies that have been misclassified. For this reason and for the possible aperture effects discussed in §4.3, a 25% fraction of young galaxies should be considered as a lower limit.

The metallicity distribution of the young, intermediate-age and old faint galaxies are shown in Fig. 10 (top panels) together with the distribution of the residuals (bottom panels) from the best fit of the relation $Z(H\beta)$ - R of Fig. 6. Old, faint galaxies have metallicities lower than -0.15 , and many of them (the majority at the faintest magnitudes) have $Z < -1$. None of them is metal-rich and their distribution of residuals has a Gaussian shape centered at $Z(\text{meas.})-Z(\text{fit})=-0.15$. This is what one expects if the best-fit relation is mostly driven by these old metal-poor galaxies and it is only slightly modified by the existence of more metal-rich (young and intermediate-age) galaxies in the same magnitude range.

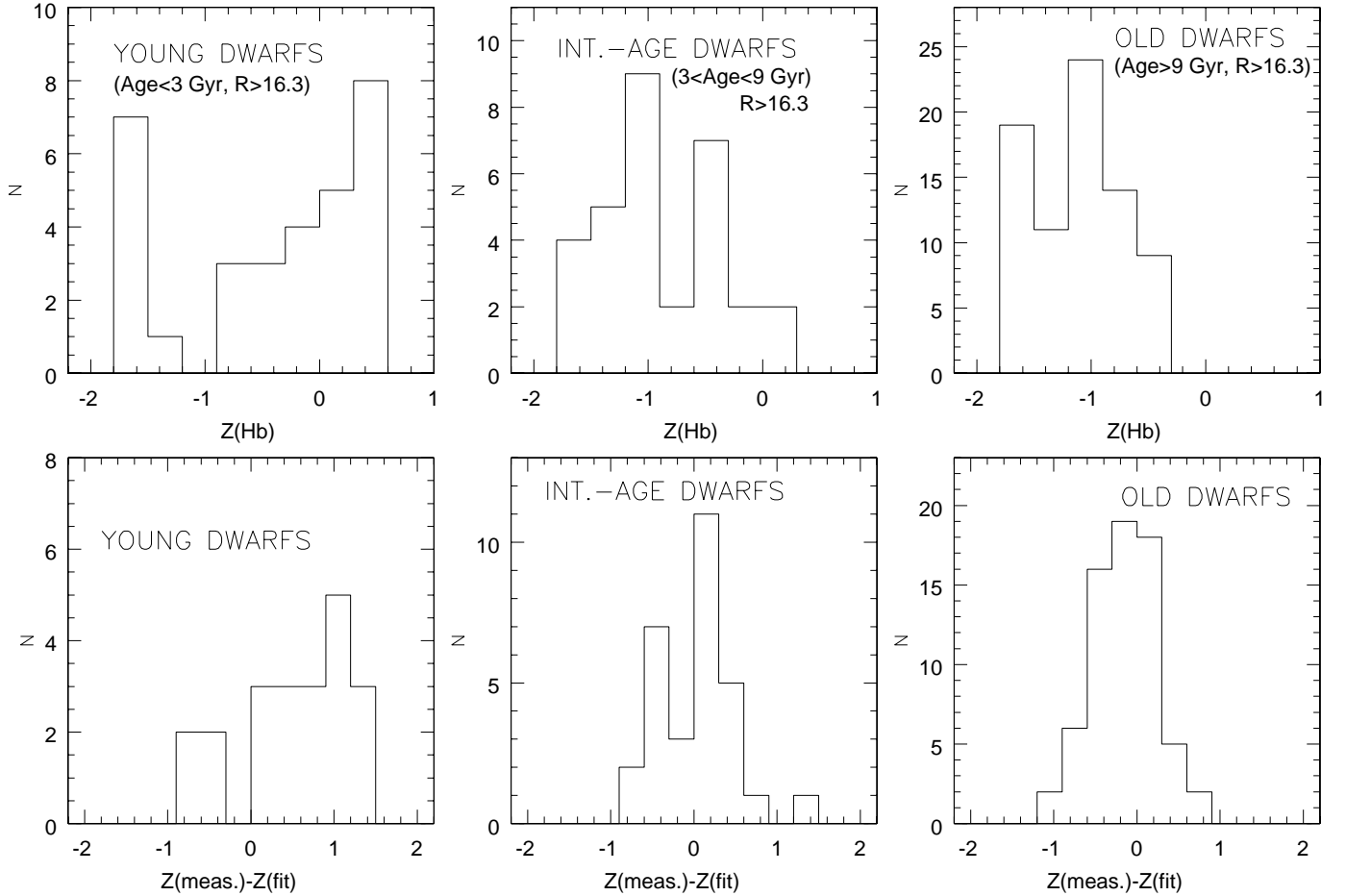


Fig. 10. Metallicity distribution (top panels) and distribution of the residuals from the best-fit line of the relation $Z(H\beta)$ - R of Fig. 6 (bottom panels). Distributions for young faint galaxies are shown in the left panels, for intermediate-age faint galaxies in the middle panels and for old faint galaxies in the right panels. Galaxies with $Z=-3/+3$ have been assigned to the bins

$Z=-1.65$ and $Z=+1.65$ respectively, and have been omitted in the plot of the residuals.

In contrast, the young faint galaxies show a bimodal metallicity distribution, a group of them being metal-rich and another group being metal-poor. The metal-rich young dwarfs are generally “too metal-rich” for their luminosity and the metal-poor ones are “too metal-poor”, as shown by the residuals plot. Being among the faintest galaxies with the lowest signal-to-noise spectra, especially below $R=18$, this result could be affected by the large errorbars in the indices, although a significant fraction of these galaxies are confirmed to be young and metal-rich also by the $H\gamma_F$ analysis.

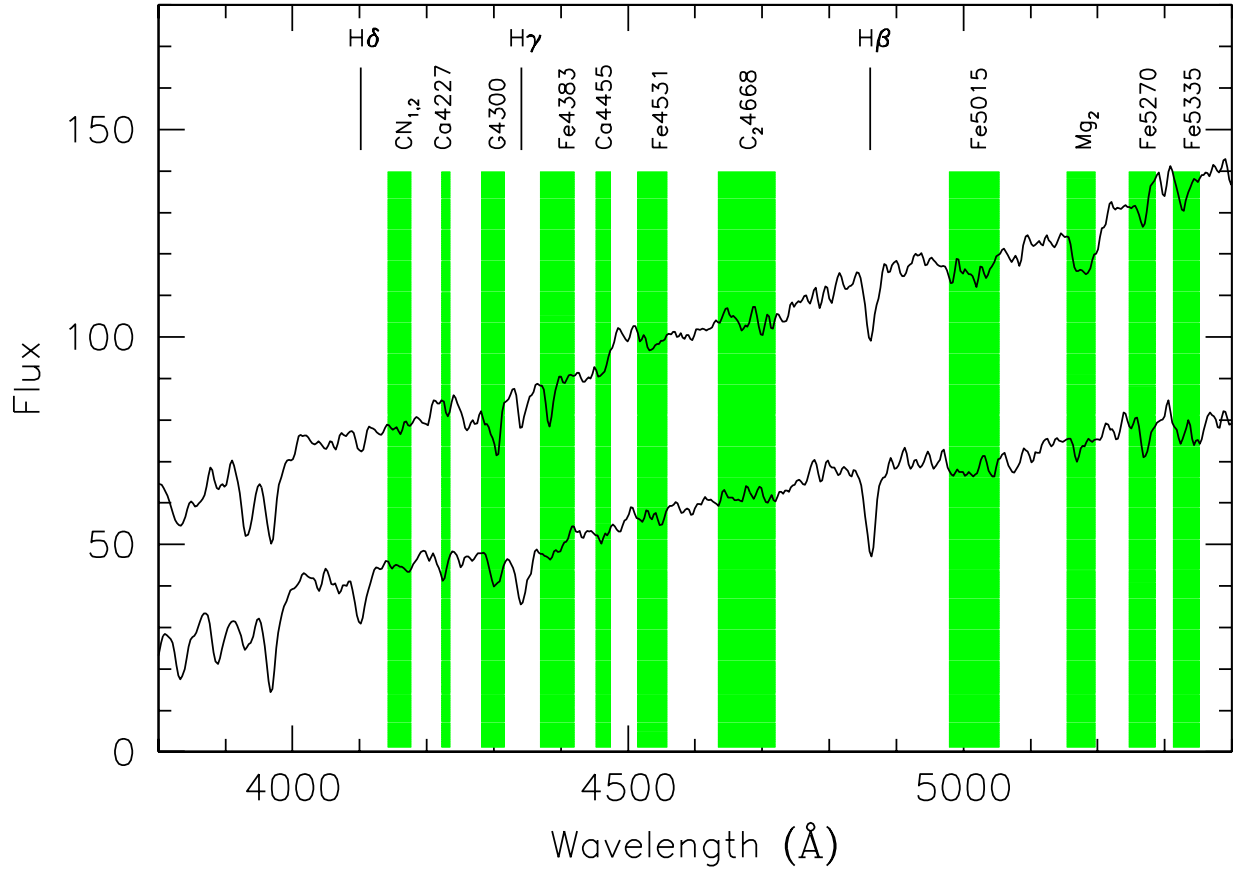


Fig. 11. Average spectra of metal-poor (lower) and metal-rich (upper) faint young galaxies as found by coadding the spectra of 7 metal-poor and 16 metal-rich dwarfs respectively ($Z < -1$ and $Z > -0.25$ in the top left panel of Fig. 10). *All but one of the metal-rich galaxies are found in Coma1, while 4 out of 7 metal-poor galaxies are in Coma3.*

In order to check the reality of these two metallicity classes, we have coadded the spectra of metal-poor and metal-rich young faint galaxies separately. The higher S/N, coadded spectra are shown in Fig. 11 and the indices measured from them are presented in Table 3. Besides the magnesium indices (on which the metal-rich vs metal-poor division is based), most of the other metallicity-sensitive indices are indeed much stronger in the average spectrum of the metal-rich young dwarfs as compared to the metal-poor coadded spectrum. This strongly supports the hypothesis of a metallicity bimodality based on the analysis of the individual lower S/N spectra (Fig. 10). However, we believe that higher signal-to-noise spectra of these galaxies will be necessary to draw definite conclusions. If confirmed, this dichotomy could point to two different formation scenarios for the faint young galaxies.

Galaxies which have been recently accreted into the cluster and have suffered from harassment (Moore et al. 1996, 1998), having lost a significant fraction of their stars, are expected to be young and unusually metal-rich for their post-harassment luminosity. Regarding this, it is interesting to note that only one out of the fifteen metal-rich (residual > 0), young dwarfs is found in the Coma3 field, while all the others are Coma1 galaxies. Another viable mechanism to form faint galaxies lying above the standard metallicity-luminosity relation is the formation of tidal dwarfs created from the tidal debris of collisions between metal-rich, massive galaxies (Duc & Mirabel 1999).

Alternatively, the existence of metal-rich Balmer-strong galaxies could be related to late evolutionary phases of *old* metal-rich populations (such as AGB-manqué stars) which are believed to be responsible for the UV-upturn below 2000 Å in luminous ellipticals (Greggio & Renzini 1990). Since this effect is not included in the stellar evolutionary models employed here¹³, in principle we cannot exclude that the Balmer-strong Mg₂-strong spectra of the dwarf galaxies which we classify as young and metal-rich are instead *old* populations whose H β index is enhanced due to old stars with metallicity much greater than solar. However, on the basis of the current models, even extremely high metallicities are not expected to be able to explain the H β values observed in our “young” metal-rich dwarfs: models of old SSPs (ages > 3 Gyr) with $Z = 1$ including hot-HB, AGB-manqué’ and Post-AGB stars only reach H $\beta = 3$ (Bressan, Chiosi & Tantaló 1996), while we observe H $\beta = 3 - 6$.

Finally, the metallicity distribution of the intermediate-age dwarfs is somewhat intermediate between that of the old and that of the young galaxies, with a broad metallicity range and possibly a composite population as well. Overall, the distributions presented in Fig. 10 testify that the mean metallicity *increases* from old to progressively younger galaxies. The existence and reality of such an age-metallicity anti-correlation for galaxies of all luminosities are the subject of the next section.

4.5. The age-metallicity anticorrelation at all magnitudes

¹³This effect must not be confused with the old *metal-poor* populations with a blue Horizontal Branch that are discussed in §3 and are already included in our models.

Galaxies in our sample follow a general trend linking age and metallicity: as displayed in Fig. 12, within a given magnitude bin younger galaxies tend to be slightly *more metal-rich* than older galaxies. The effect is more evident for bright galaxies whose relations show less scatter.

Several previous studies found evidence for a similar age-metallicity anti-correlation (Faber et al. 1995, Worthey et al. 1995, Gorgas et al. 1997, Trager 1997, Worthey 1997, Kuntschner & Davies 1998, Trager et al. 1998, Colless et al. 1999, Ferreras, Charlot & Silk 1999, Jorgensen 1999, Saglia et al. 1999, Terlevich et al. 1999, Longhetti et al. 2000, Trager et al. 2000b, Kuntschner 2000, Kuntschner et al. 2001, Rakos et al. 2001) and it has been suggested that this “conspiracy” could contribute to the tightness of the global relations (e.g. the index-magnitude relations) such that deviations due to age can be counter-balanced by metallicity effects (e.g. Faber et al. 1995, Worthey et al. 1995, Trager 1997, Jorgensen 1999, Trager et al. 2000b).

The reality of such an age-Z anti-correlation is hard to establish, due to the fact that errors in the Z-index versus age-index diagram are correlated: as shown by Trager et al. (2000b) and Kuntschner et al. (2001), an error in a Z-index, for example, produces an error in both the age and the metallicity estimate, in the sense that if the age is underestimated then the metallicity is overestimated, and vice-versa. As a result, a spurious anti-correlation between age and metallicity is produced. Index measurements with small errors (i.e. high S/N spectra) are required to feel confident that the anticorrelation is not just due to correlated errors (Trager et al. 2000b); for the youngest five galaxies in their sample, Kuntschner et al. (2001) conclude that they are indeed more metal-rich than the average galaxy and therefore at least in these cases the age-Z anticorrelation is real.

Although we believe at the moment this is an open issue, we note that if correlated errors were the cause then the effect would be expected to be more evident in the lowest S/N subset of our sample, i.e. at the faintest magnitudes. This is not the case, on the contrary the anticorrelation is best observed among the brightest subset of galaxies (Fig. 12), whose mean error on $H\beta$ is only 0.16 \AA . This mild anticorrelation corresponds to clearly visible differences in the metallicity distribution of bright galaxies of different ages (Fig. 13). Comparing this with the Z distributions of the dwarfs (Fig. 10), it is the small group of *metal-poor* young dwarfs which is “anomalous”, and deviates from the general trend.

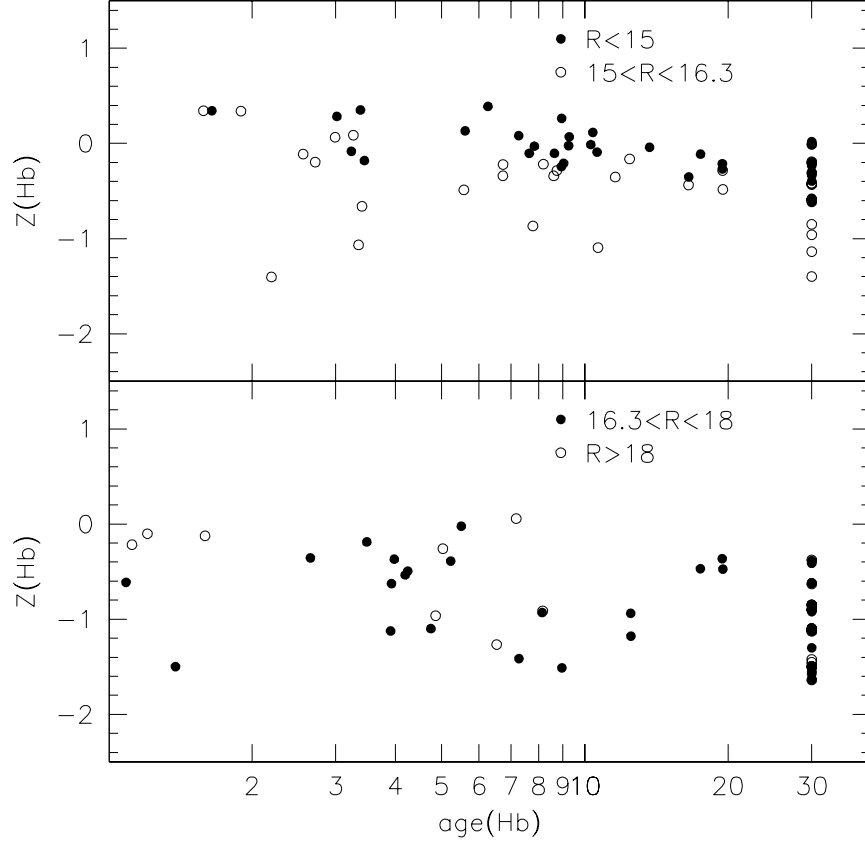


Fig. 12. Ages versus metallicities of Coma1 galaxies as derived from the $H\beta/Mg_2$ diagram. The best-fit relations in the top panels are $Z=0.445 - 0.461 \times \log(\text{age})$ ($R < 15$) and $Z=0.051 - 0.4 \times \log(\text{age})$ ($15 < R < 16.3$).

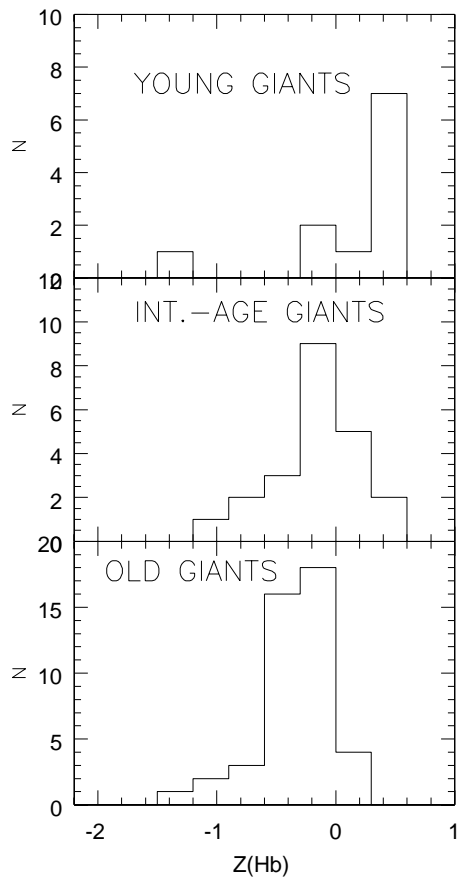


Fig. 13. Metallicity distributions of young, intermediate-age and old giants ($R < 16.3$) in Coma1.

4.6. The slope, the scatter and the outliers of the index-magnitude relations

Once we have determined the ages and metallicities of each galaxy as described above, we can investigate the origin of the index-magnitude relations (Fig. 3). In particular, we wish to understand what determines the slope and the scatter of these relations and what are the properties of the outliers that lie above the general trend. Hereafter the discussion will be limited to ages and metallicities derived from the $H\beta$ - Mg_2 diagram, which have smaller errorbars than $H\gamma_F$ - $\langle Fe \rangle$.¹⁴

The location in the index- R diagram of the various age and metallicity classes defined in §4.3 is shown in Figs. 14 and 15. We first note that, if the measured errors are not significantly underestimating the true

¹⁴Conclusions similar to those presented in this section are reached using the $H\gamma_F$ index instead of $H\beta$ and $\langle Fe \rangle$ instead of Mg_2 .

errors, the fact that the observed scatter is larger at fainter magnitudes should be only partly due to the increasing uncertainties in the index measurements: the *intrinsic* scatter is shown by the vertical segments for four magnitude bins and it is larger for fainter galaxies.

In Fig. 14a, it is evident how the old, intermediate-age and young galaxies segregate in the $H\beta$ -R plot. Considering for the moment only old galaxies, their upper envelope traces a correlation between the strength of the $H\beta$ index and magnitude. The existence of this relation is a metallicity effect not related to age. In fact, the value of the $H\beta$ index of *the old galaxies* lying on the index-magnitude relation is anticorrelated with Z and has no correlation with age (Fig. 16). The presence of intermediate-age and young galaxies in this plot produces a thickening in the $H\beta$ -R relation at bright magnitudes and a slight shift in the zero point towards stronger $H\beta$, while young galaxies are responsible for the outliers lying above the relation, mostly at faint magnitudes. However, it can be seen in Fig. 15a that a relation between $H\beta$ and R persists even when only galaxies in a certain metallicity range are considered. For example, the existence of the relation $H\beta$ -R for metal-rich galaxies is an age effect, with fainter galaxies being on average younger. No obvious age segregation is instead visible in the Mg_2 -R plot (Fig. 14b).

Turning to the location of galaxies with different metallicities, they largely segregate in the Mg_2 -R diagram (Fig. 15b), going from higher indices (the metal-rich galaxies) to progressively lower indices (intermediate- Z and metal-poor galaxies), with some overlap in the index range of the three classes. Considering one metallicity class at a time, for example the metal-rich galaxies, we observe that they still display a trend with R : such a relation is an age effect (fainter galaxies being on average younger than bright galaxies within the same metallicity class), as proved by the fact that the Mg_2 index of *the metal-rich galaxies* – or, equivalently, another metallicity class – is correlated with age and not with Z (Fig. 16). The Mg_2 -R relation traced by the metal-rich galaxies has a slope similar to that of the *global* relation produced by all three metallicity classes together, which is shown as a solid line in Fig. 15b. If the trend of decreasing mean age with magnitude did not exist, the Mg_2 -R relation of the metal-rich galaxies would be flat. However, a global Mg_2 -R relation would still exist, due to the different index and magnitude distributions of metal-rich, intermediate and metal-poor galaxies. Strictly speaking, the relation would exist – with a larger scatter – even if only one of the trends with magnitude, either that of the mean age or that of the mean Z , were in place. The fact that both trends are present makes the relation *tighter*, especially at faint magnitudes.

To conclude, the characteristics of the index-magnitude relations (slope, zero-point, scatter and outliers) are the result of both age and metallicity trends with magnitude which are intertwined in an intricate manner. Similarly to the color-magnitude relation of early-type galaxies (Bower, Lucey & Ellis 1992; Kodama & Arimoto 1997; Kauffmann & Charlot 1998; Kodama et al. 1998; Terlevich et al. 1999), a dominant factor appears to be metallicity, which is able to largely account for the slope of the indices-R relations, hence would be sufficient to produce index-R relations similar to the ones observed even if the trend of decreasing mean age with magnitude did not exist. Nevertheless, the spread in ages cannot be neglected if one wants to understand in detail the characteristics of these relations (slopes, zero-point, scatter) and the outliers. Finally, it is natural to wonder how the variety of star formation histories observed in the present sample and presented in §4.3 can give rise to relatively tight index-magnitude relations. In a sense this is not surprising, since metallicity turns out to be the dominant effect in determining the slope of the relations, and given the existence of the Z -luminosity relation. Hence, the correct way to address this question is to aim at understanding the reason for the Z dependence on L even in galaxies with different star formation histories, as discussed in §4.3.

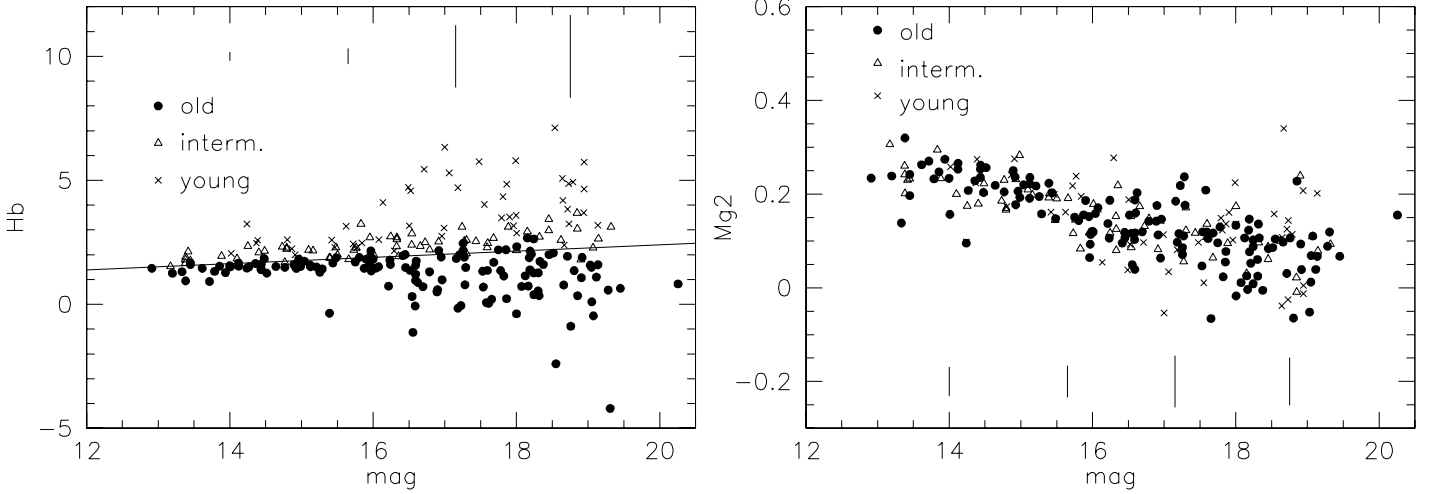


Fig. 14. Index-magnitude relations as in Fig. 3 for old (age > 9 Gyr), intermediate-age (between 3 and 9 Gyr) and young (age < 3 Gyr) galaxies. Both Coma1 and Coma3 galaxies are included. The straight line in the left panel is the best fit given in Table 2 and shown also in Fig. 3. The values of the intrinsic scatter in four magnitude bins are shown as vertical segments. The intrinsic scatter has been computed as $\sigma_{intr.}^2 = (y - B \times R - A)^2 - \sigma_y^2$, where $y = A - B \times R$ is the observed best-fit relation between the index y and the magnitude R (Fig. 3) and σ_y^2 is the measured error on the index.

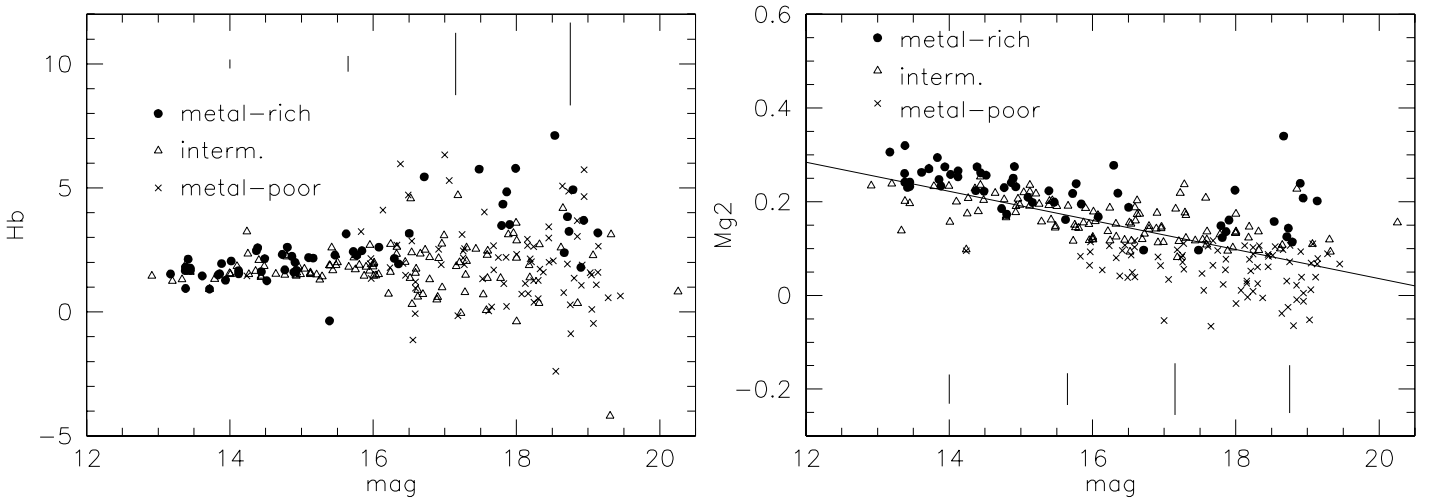


Fig. 15. Index-magnitude relations as in Fig. 3 for metal-rich ($Z > -0.15$), intermediate- Z ($-1 < Z < -0.15$) and metal-poor

($Z < -1$) galaxies. Both Coma1 and Coma3 galaxies are included. The straight line in the right panel is the best fit given in Table 2 and shown also in Fig. 3. The values of the intrinsic scatter in four magnitude bins are shown as vertical segments.

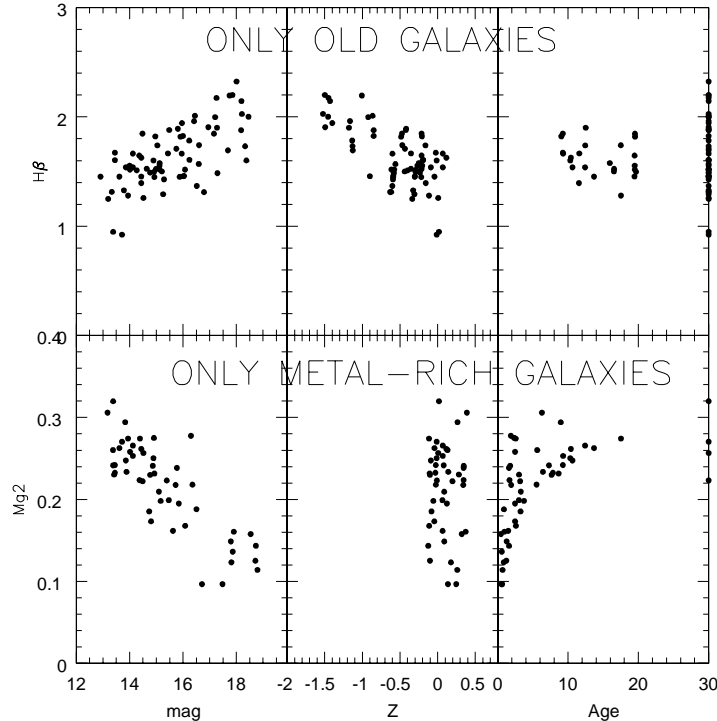


Fig. 16. Top panels. $H\beta$ index versus magnitude, versus metallicity and versus age for old galaxies lying on the index-magnitude relation only. Bottom panels. Mg_2 index versus magnitude, versus metallicity and versus age for metal-rich galaxies only.

5. Conclusions

Analysis of the Lick indices of a large sample of Coma galaxies with $-20.5 < M_B < -14$ has shown systematic trends of the index values with both galaxy luminosity and environment (Fig. 2). In this paper we have investigated the properties of the non-emission-line galaxies and focussed on the relations between index strength and luminosity, with the aim of understanding the origin of the mean relations, the cause of their scatter and the properties of the outlying points. The derived distributions of luminosity-weighted ages and metallicities provide some important indications about the evolutionary history of cluster galaxies as a function of galactic luminosity.

The main results can be summarized as follows:

a) In our sample all the Lick indices sensitive to metallicity (Mg_2 , $\langle Fe \rangle$, C_{24668} etc.) display a correlation with luminosity, and all the age-sensitive indicators (Balmer indices) anticorrelate with

luminosity. For the first time, we find that all these relations hold also for faint, non-emission line galaxies, down to $M_B \sim -14$.

b) By comparing the observed indices with model grids based on the Padova isochrones, we derive luminosity-weighted ages and metallicities. In doing this, we find a large number of faint galaxies whose Balmer indices are too low to be explained by the current models. Interestingly, this phenomenon has also been previously observed in the spectra of several globular clusters, even at high signal-to-noise. Moreover, on the basis of the random errors and given the spectral characteristics of this sample, observational errors and/or eventual emission filling of the Balmer lines do not seem sufficient to explain the observed population of faint galaxies with low Balmer lines. A possible reason for the discrepancy between the indices measured and the model grids is an overestimate of the turn-off temperature in the models, hence we tentatively interpret the galaxies with very low Balmer indices as old stellar systems (age > 9 Gyr).

c) The mean metallicity increases with galaxy luminosity. The spread in metallicity at a given magnitude is large, especially for galaxies fainter than $M_B \sim -18$. This spread is larger than the nominal scatter due to the random errors in the index measurements, although it should be kept in mind that additional sources of errors (such as cosmic rays and sky residuals) have not been included.

d) A broad range of ages, from younger than 3 Gyr to older than 9 Gyr, is found in galaxies of any magnitude but a large fraction of the currently non-star-forming galaxies of *any* luminosity (dwarfs and giants) are devoid of signs of star formation occurred at $z < 2$. This fraction is found to be $\sim 50\%$ at all magnitudes, but it is more uncertain and could be as low as 30% for the dwarfs. Although no clear correlation is observed between age and magnitude, there are systematic trends between the “luminosity-weighted” epoch of the most recent star formation episode and luminosity. At $z < 0.35$, the star formation activity has involved a higher proportion of faint galaxies (at least 20% of the present-day population) than bright ones ($\sim 5\text{-}10\%$). Using the derived ages at face value, the fraction of present-day luminous galaxies with significant star formation at intermediate redshifts ($0.35 < z < 2$) is higher than the fraction of present-day faint galaxies that were active at that epoch (30-50% against 15-25%), but this last result could be affected by the large errorbars on the indices of the dwarfs.

e) The metallicity distributions of faint galaxies with young luminosity-weighted ages (< 3 Gyr) and, possibly, those with intermediate-age (3-9 Gyr) are bimodal, with a group being “too metal-rich” and another group being “too metal-poor” with respect to the mean metallicity at their magnitude. This bimodality is also supported by the index strengths obtained coadding the spectra of the two groups of galaxies separately. This is suggestive of two separate mechanisms for the formation of the faint galaxy population in clusters, but we stress that this result needs to be confirmed by higher signal-to-noise spectra of a large number of galaxies at the faintest magnitudes.

f) An anticorrelation between age and metallicity is found among galaxies in any given luminosity bin. This could be spuriously produced by the fact that the errors in the derivation of the age and the metallicity are correlated, but the fact that the age-metallicity anticorrelation is best observed in the subset of galaxies with the highest signal-to-noise spectra seems to suggest that it is real.

g) An interpretation of the observed index-magnitude relations is presented. Both age and metallicity variations as a function of luminosity play a role in determining the characteristics of the index-magnitude relations (slope, scatter, zero-point and outliers). The relations are the consequence of both age and metallicity trends with luminosity: each such trend on its own would be sufficient to produce relations qualitatively similar (and not too different in slope) to those observed.

Acknowledgements

We are sincerely grateful to Herve’ Aussel who wrote for us the IDL program that convolves the spectra with a wavelength-dependent Gaussian. We thank the referee, Dr. Guy Worthey, for his useful comments which gave us an opportunity to improve the paper. We also thank Matthew Colless for providing us with his spectroscopic catalog of Coma galaxies and for assistance throughout this project. This research has greatly benefited from the availability of the PhD theses of Nicolas Cardiel Lopez (University of Madrid), Harald Kuntschner (University of Durham), Marcella Longhetti (University of Milano) and Scott C. Trager (University of California, Santa Cruz). We acknowledge helpful discussions with and/or comments about this manuscript from Cesare Chiosi, Fabio Governato, George Hau, Enrico Held, Harald Kuntschner, Ian Smail, Scott Trager, Alexandre Vazdekis and Guy Worthey, and we thank the latter two colleagues for maintaining very useful WEB pages of their models. This research has made use of the NASA/IPAC Extragalactic Database (NED) which is operated by the Jet Propulsion Laboratory, Caltech, under contract with the National Aeronautics and Space Administration.

Appendix A: Measurements of the Lick indices

a) *Spectral resolution.* The Lick/IDS spectral resolution varies with wavelength as described in WO97 (see also Fig. A1). The resolution of our spectra has been estimated from the arc exposures and has been found to vary only slightly with wavelength; at each given wavelength, the resolution stays approximately constant within the “internal fibres” (fibre numbers 30-110) and worsens progressively in the “external fibres” (< 30 and > 110) towards the edges of the chip. Fig. A1 presents the mean FWHM¹⁵ of the internal and external fibres found as a polynomial interpolation of the FWHM at 4158, 4695, 5606 and 6416 Å. We have broadened our internal and external spectra with a Gaussian of wavelength dependent width, in such a way to match the Lick/IDS resolution *at the observed λ corresponding to the rest-frame λ of the Lick/IDS system* ($\lambda_{\text{observed}} = (1 + z) \lambda_{\text{Lick}}$). For cluster members this was done assuming a common redshift $z = 0.023$; the fore/background galaxies were divided into redshift bins and the Gaussian convolution was done for each redshift bin at the appropriate wavelength. In this way, we have degraded our spectra to a spectral resolution which is the same of the Lick spectra at each spectral index. After Gaussian convolving and deredshifting the spectra, the indices were measured using the IRAF-*sbands* tool (see Appendix B).

¹⁵We have verified that the variation of the resolution within the group of external fibres is small enough not to affect the results.

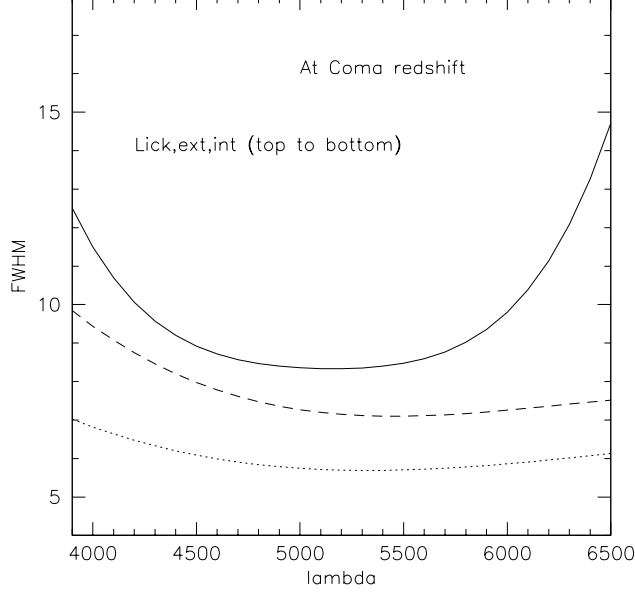


Fig. A1. Spectral resolution of the Lick spectra (solid line), of our external-fibre spectra (long dashed line) and of our internal-fibre spectra (dotted line) at the wavelengths observed at the Coma redshift.

b) *Velocity dispersion correction.* The line-of-sight velocities of the stars in a galaxy broaden the spectral features of its integrated spectrum; in contrast, the model integrated spectrum simply adds up the contribution of all stars, hence in order to compare with the Lick models it is necessary to correct the values of the observed indices to a zero-velocity dispersion.

Velocity dispersions for 23 giant galaxies in our sample are available from Lucey et al. (1997). Following Terlevich et al. (1999), we constructed the relation between these velocity dispersions and our R band magnitudes and used the fit to this relation to estimate the velocity dispersion of the rest of the galaxies. This relation is expected to be valid for luminous galaxies, while the behaviour of the σ -Luminosity relation for dwarf galaxies is not well determined. Hence, a $\sigma = 50 \text{ km s}^{-1}$ was assigned to those faint galaxies for which the relation described above yields $\sigma < 50 \text{ km s}^{-1}$. Given our spectral resolution, the velocity dispersion correction for dwarf galaxies is negligible.

At the telescope we obtained 12 usable spectra of 5 different stars of the Lick/IDS stellar library (HR2002, HR2600, HR3262, HR3427, HR3905). After having convolved the flux-calibrated stellar spectra with a wavelength-dependent Gaussian as described at point a), we further broadened the spectra with a Gaussian filter to mimic a “galaxy velocity dispersion” in the range $\sigma = 30 - 310 \text{ km s}^{-1}$ in steps of 20 km s^{-1} . We have then measured the indices for each star and each σ and found the mean correction factors $C^I(\sigma) = \text{Index}(0)/\text{Index}(\sigma)$ (atomic indices) and $C^I(\sigma) = \text{Index}(0) - \text{Index}(\sigma)$ (molecular indices) that are presented in Fig. A2. The indices correction factors of each galaxy were computed from the galaxy velocity dispersion linearly interpolating between points in Fig. A2.

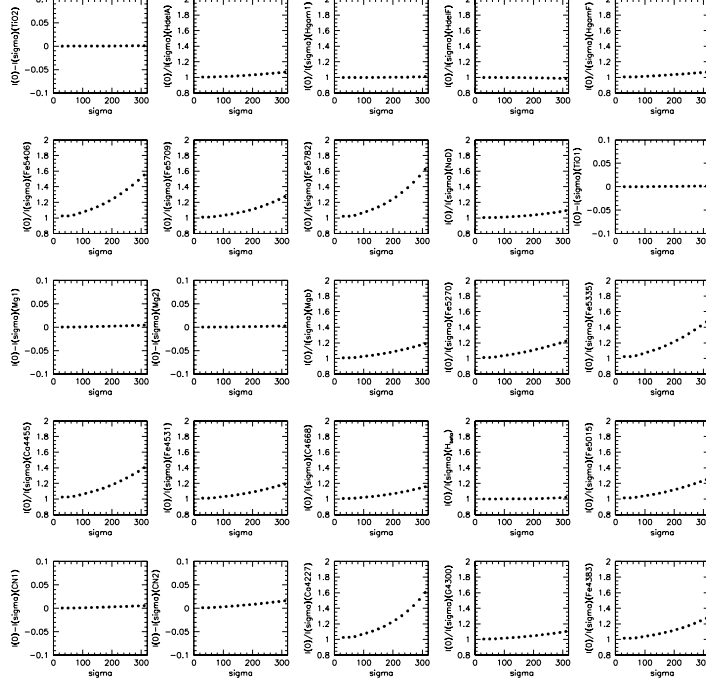


Fig. A2. Correction factors as a function of the galaxy velocity dispersion. Corrections are highest for narrow atomic indices, such as the Fe indices.

c) *Offsets.* The Lick spectra were not flux calibrated, but normalized to a quartz-iodide tungsten lamp, therefore we need to correct for the small systematic offsets produced by the different continuum shape. We have measured the Lick indices of the flux-calibrated stellar spectra (after performing the wavelength-dependent Gaussian convolution described at point a) and compared them with the values given in the Lick papers (WO97). The mean offsets between our and Lick measurements are listed in Table A1; our index values have been corrected for these offsets only if the offset was bigger than its 1σ error.

Appendix B: Tests of the Lick/IDS calibration

The comparison of our measured indices with model predictions relies on a careful calibration onto the Lick/IDS system. We have assessed the accuracy of this calibration in a number of ways:

a) *Index measuring routine.* we have verified that the method we adopted for measuring the indices (the IRAF-sbands tool) reproduces the index values measured by the Lick team. For allowing colleagues to test their measuring routine, Guy Worthey provides on his WEB page the spectra and Lick indices of 8 test-stars; the agreement between our measurements and those of Lick is excellent and gives a mean relative error of $0.5 \pm 0.4\%$.

b) *Comparison with the Lick index measurements.* The Lick/IDS galaxy library includes 5 Coma

TABLE 3
INDICES MEASURED ON THE COADDED SPECTRA

Index	Bandpass	Metal-poor	Metal-rich	MR>MP ?
CN ₁		-0.123±0.017	-0.054±0.015	+
CN ₂		-0.091±0.020	-0.027±0.016	+
Ca4227		0.667±0.143	0.588±0.133	-
G4300		1.576±0.497	5.864±0.378	+
Fe4383		0.848±0.544	3.119±0.455	+
Ca4455		0.675±0.232	1.596±0.236	+
Fe4531		1.377±0.329	2.366±0.221	+
C ₂ 4668		1.103±0.574	1.222±0.652	+
Fe5015		3.581±0.827	4.128±0.227	+
Mg ₁		0.010±0.018	0.049±0.007	+
Mg ₂		0.003±0.007	0.160±0.004	+
Mgb		0.790±0.191	2.735±0.123	+
Fe5270		2.162±0.358	1.491±0.063	-
Fe5335		1.600±0.228	1.984±0.098	+
Na D		-0.507±0.318	1.325±0.125	+

Sky-lines contamination (OI5577,NaD5890/6,OI6302) affects Fe5406, 5709,5782,TiO₁ and TiO₂, which have been omitted from this table. Errors have been computed from the index differences of various “Monte-carlo” combinations of metal-poor and metal-rich spectra.

TABLE A1
SYSTEMATIC OFFSETS

Index	Offset (This work-Lick)
CN ₁	0.018±0.011
CN ₂	0.016±0.016
Ca4227	-0.028±0.109
G4300	0.123±0.291
Fe4383	-0.316±0.172
Ca4455	-0.260±0.136
Fe4531	0.088±0.334
C ₂ 4668	0.014±0.349
H _β	0.038±0.090
Fe5015	-0.362±0.313
Mg ₁	0.015±0.028
Mg ₂	0.011±0.012
Mgb	-0.017±0.109
Fe5270	-0.288±0.149
Fe5335	-0.119±0.245
Fe5406	-0.055±0.155
Fe5709	-0.071±0.135
Fe5782	-0.073±0.095
Na D	-0.176±0.105
TiO ₁	0.003±0.003
TiO ₂	0.015±0.011
Hδ _A	0.330±0.371
Hγ _A	-0.137±0.332
Hδ _F	0.107±0.157
Hγ _F	-0.038±0.126

galaxies in common with our sample (Trager et al. 1998, Worthey in prep.). The galaxy area covered by our fibre diameter (2.7 arcsec) matches quite well the Lick/IDS standard aperture (1.4×4 arcsec), hence we check the consistency with the Lick/IDS system comparing directly our and their measurements in Fig. B1. The figure shows a good general agreement within the errors.

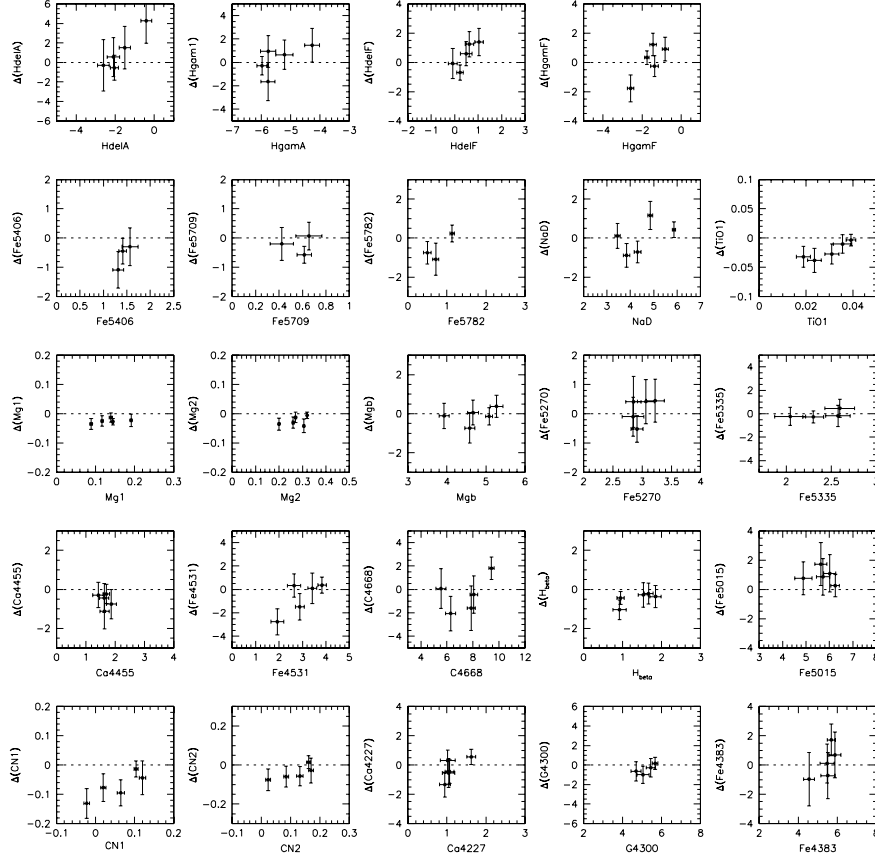


Fig. B1. Differences $\Delta = (\text{This Work} - \text{Lick})$ between our and Lick (Trager et al. 1998, Worthey in prep.) index measurements for the 5 giant galaxies in common versus our index measurements. Some of the plots contain less than 5 galaxies when a measurement was missing in the Lick list. The TiO₂ plot is missing because this index was not measured by Lick for any of these galaxies.

c) *Comparison with Jorgensen's index measurements.*

Recently, Jorgensen (1999, J99) published $H\beta$, Mg_1 , Mg_2 , Mgb and $\langle Fe \rangle$ indices of a large sample of E and S0 galaxies in Coma. The index measurements of the 16 galaxies in common are compared in Fig. B2 (circles). Jorgensen's spectroscopic parameters are centrally measured values corrected to a circular aperture of diameter $1.19 h^{-1}$ kpc (see J99 for details), therefore we expect at least part of the differences to be due to aperture effects. The agreement in Fig. B2 is satisfactory, but we note a possible anticorrelation between the index differences and the index strength for Mg_2 and - to a minor extent - Mg_1 and $H\beta$. To investigate the origin of this behaviour, in Fig. B2 we also plot as crosses the differences between Jorgensen's

and Trager’s measurements of the 5 common galaxies: as expected from the agreement between Trager’s and our measurements found in Fig. B1, the differences J-T follow the same trend as the differences between J99 and this work. The source of this systematic trend could be related to the dissimilar apertures, but a detailed investigation of the discrepancy is beyond the scope of this work and we do not discuss it further.

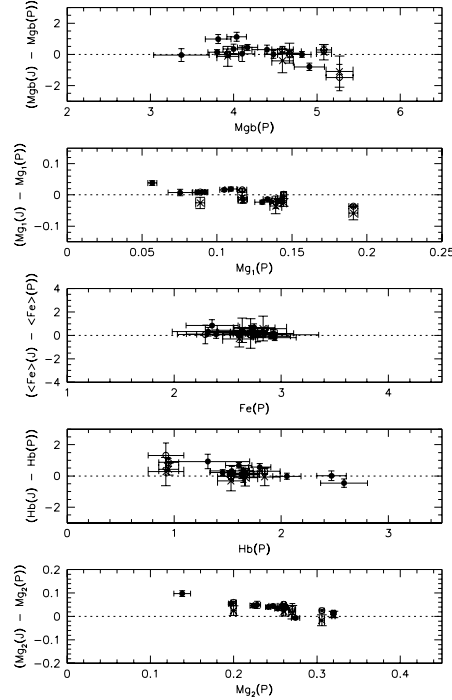


Fig. B2. Differences between Jorgensen’s (1999) and our (P) measurements for the 16 giant galaxies in common. Empty circles identify those 5 galaxies in common among Trager, Jorgensen and this work. The crosses mark the differences between Jorgensen and Trager measurements of the common galaxies (see text for details).

d) *Index-index plots for indices dominated by similar species.*

The consistency of the calibration onto the Lick system and with the model predictions can be investigated by means of index-index plots which present indices that are sensitive to the same chemical species (Kuntschner 2000). In these plots the model predictions should closely follow the relation traced by the data. There are three main families of indices (Trager et al. 1998): 1) α -element indices (CN, Mg, NaD, TiO2); 2) Fe-like indices (Ca, G band, TiO1, all Fe indices); ¹⁶ 3) Balmer indices.

Here we only consider those indices that are used in this paper for deriving ages and metallicities: their index-index plots are presented in Fig. B3 (lower panel of each plot). For comparison, the upper panel of each plot displays the data of the Lick galaxies (dots) and globular clusters (crosses). Note that the errorbars for our giant sample are considerably smaller than the mean errors in the Lick/IDS sample of galaxies (see §4.2), while our dwarf galaxy errors are larger. The position of our giant galaxies in the

¹⁶C₂4668 has been shown by Trager et al. (1998) to be somewhat intermediate between the α and Fe groups.

diagrams overlap with the positions of the Lick (giant) galaxies, but our sample does not reach the highest metallicity-indices values observed in the Lick sample, because of the different galaxy luminosity ranges. Dwarf galaxies span a wide range in all indices and they also occupy the region of the diagrams where the Lick globular clusters are found. The models generally trace well the relations where the data lie, with the well known exception of the Mg indices due to the enhanced Mg/Fe ratio of the luminous galaxies. These model deviations are observed in both the lower and the upper panels of Fig. B3, as well as in any other sample (e.g. Kuntschner 2000).

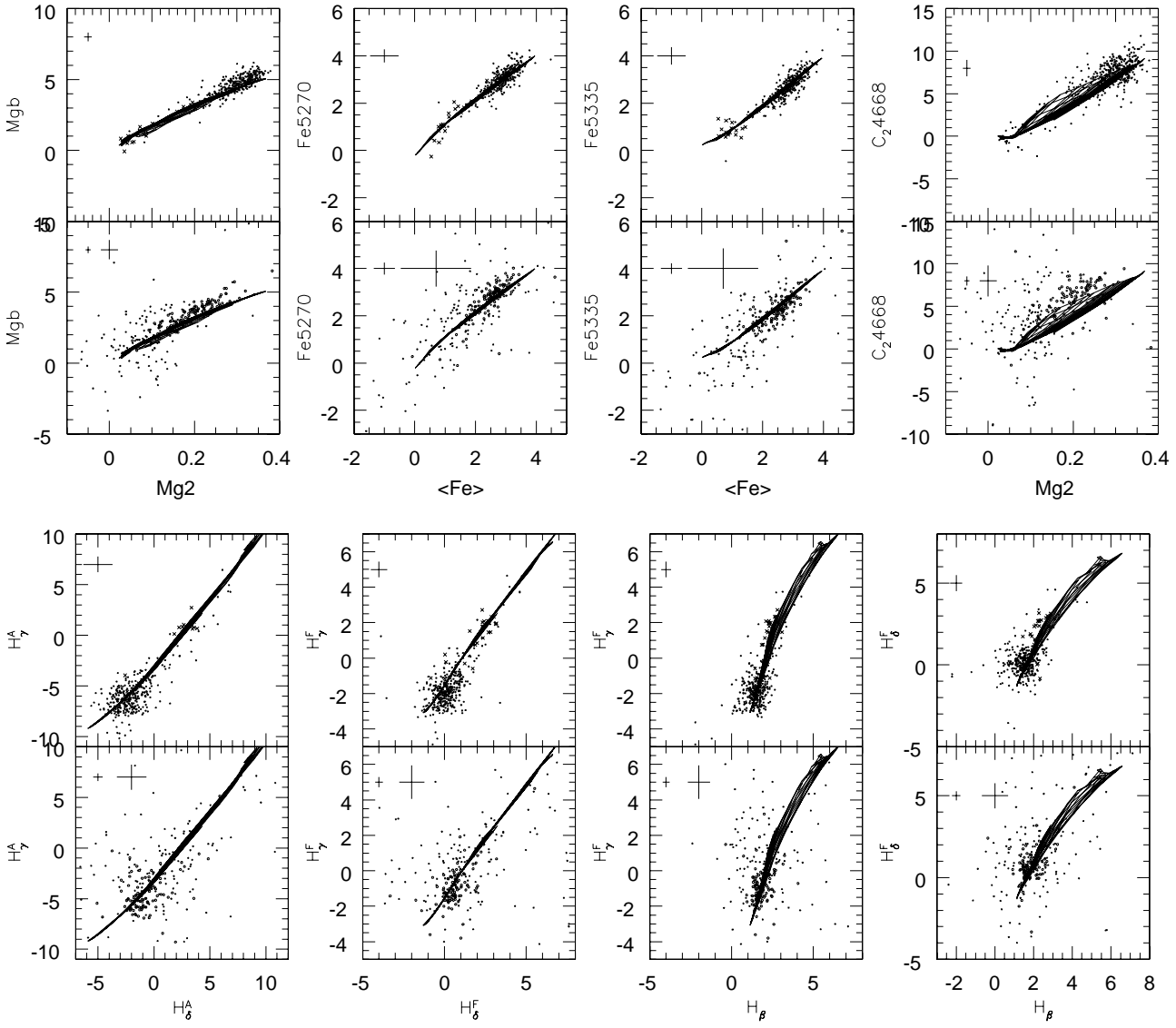


Fig. B3. Index versus index plots of indices dominated by the same chemical species. Our whole galaxy sample is shown in the lower panel of each plot: filled dots are dwarfs and empty dots are giants. Galaxies with emission lines have been excluded from this figure. The upper panel of each plot presents the Lick/IDS sample (Trager et al. 1998, Worthey in prep.) of galaxies (filled dots) and globular clusters (crosses). The median errorbars of our giant (left) and dwarf (right) galaxies are shown in the upper left corner of the lower panels. The median errorbar of the Lick galaxies is in the upper left corner of the upper panels. Overplotted are Worthey’s models (see text).

REFERENCES

- Babul, A., Rees, M. J., 1992, MNRAS, 255, 346
- Barger A. J., Aragon-Salamanca A., Ellis R. S., Couch W. J., Smail I., Sharples R. M., 1996, MNRAS, 279, 1
- Bender, R., Burstein, D., Faber, S. M., 1993, ApJ, 411, 153
- Bender, R., Ziegler, B., Bruzual, G., 1996, ApJ, 463, 529
- Bender, R., Saglia, R. P., Ziegler, B., Belloni, P., Greggio, L., Hopp, U., 1998, ApJ, 493, 529
- Bertelli, G., Bressan, A., Chiosi, C., Fagotto, F., Nasi, E., 1994, A&AS, 106, 275
- Bothun, G. D., Mould, J. R., Wirth, A., Caldwell, N., 1985, AJ, 90, 697
- Bothun, G. D., Mould, J. R., 1988, ApJ, 324, 123
- Bower, R. G., Ellis, R. S., Rose, J. A., Sharples, R. M., 1990, AJ, 99, 530
- Bower, R. G., Lucey, J. R., Ellis, R. S., 1992, MNRAS, 254, 601
- Bressan, A., Chiosi, C., Tantalo, R., 1996, A&A, 311, 425
- Brodie, J. P., Huchra, J. P., 1991, ApJ, 379, 157
- Burstein, D., Faber, S. M., Gaskell, C. M., Krumm, N., 1984, ApJ, 287, 586
- Burstein, D., Davies, R. L., Dressler, A., Faber, S. M., Lynden-Bell, D., Terlevich, R. J., Wegner, G., 1988, in Towards Understanding Galaxies at Large Redshifts, eds. Kron R. G., & Renzini, A., Kluwer, Dordrecht, p.17
- Butcher, H., Oemler, A. Jr. 1978, ApJ, 226, 559
- Butcher, H., Oemler, A. Jr. 1984, ApJ, 285, 426
- Buzzoni, A., 1995, ApJS, 98, 69
- Caldwell, N., 1983, AJ, 88, 804
- Caldwell, N., Bothun, G. D., 1987, AJ, 94, 1126
- Caldwell, N., Rose, J. A., Sharples, R. M., Ellis, R. S., Bower, R. G., 1993, AnJ, 106, 473
- Caldwell, N., Rose, J. A., 1997, AnJ, 113, 492
- Caldwell, N., Rose, J. A., 1998, AJ, 115, 1423
- Caldwell, N., 1999, AnJ, 118, 1230
- Cardiel, N., PhD Thesis, University of Madrid
- Cardiel, N., Gorgas, J., Cenarro, J., González, J. J., 1998, A&AS, 127, 597
- Cohen, J. G., Blakeslee, J. P., Ryzhov, A., 1998, ApJ, 496, 808
- Colless, M., Burstein, D., Davies, R. L., McMahan, R. K., Saglia, R. P., Wegner, G., 1999, MNRAS, 303, 813
- Concannon, K. D., Rose, J. A., Caldwell, N., 2000, ApJL, 536, L19
- Couch W. J., Sharples R. M., 1987, MNRAS, 229, 423 (CS87)
- de Carvalho, R. R., Djorgovski, S., 1992, ApJ, 389, L49
- Dekel, A., Silk, J., 1986, ApJ, 303, 39
- Dressler A., Gunn J. E., 1982, ApJ, 263, 533
- Dressler A., Gunn J. E., 1983, ApJ, 270, 7
- Dressler, A., 1984, ApJ, 281, 512

- Dressler, A., Lynden-Bell, D., Burstein, D., Davies, R. L., Faber, S. M., Terlevich, R. J., Wegner, G., 1987, *ApJ*, 313, 42
- Dressler A., Gunn J. E., 1992, *ApJS*, 78, 1
- Dressler, A., Smail, I., Poggianti, B. M., Butcher, H., Couch, W. J., Ellis, R. S., Oemler, A., 1999, *ApJS*, 122, 51
- Duc, P.-A., Mirabel, I. F., 1999, in *Galaxy interactions at high and low redshift*, IAU Symp. 186, eds. J. Barnes & D. B. Sanders, Kluwer, Dordrecht
- Efstathiou, G., 1992, *MNRAS*, 256, 43
- Faber, S. M., 1973, *ApJ*, 179, 423
- Faber, S. M., Trager, S., González, J., Worthey, G., 1995, in *Stellar Populations*, IAU Symp. n.164, eds. van der Kruit & Gilmore, Kluwer, Dordrecht, p.249
- Ferguson, H. C., 1994, in *Dwarf Galaxies*, ESO Conf. Proc. N.49, eds. Meylan & Prugniel, Haute-Provence, ESO, p.475
- Ferguson, H. C., Binggeli, B., 1994, *A&AR*, vol.6, p.67
- Ferreras, I., Charlot, S., Silk, J., 1999, *ApJ*, 521, 81
- Fisher, D., Franx, M., Illingworth, G., 1996, *ApJ*, 459, 110
- Forbes, D. A., Ponman, T. J., Brown, R. J. N., 1998, *ApJ*, 508, L43
- Forbes, D. A., Ponman, T. J., 1999, *MNRAS*, 623, 628
- Gibson, B. K., Madgwick, D. S., Jones, L. A., Da Costa, G. S., Norris, J. E., 1999, *AnJ*, 118, 1268
- González, J. J., 1993, PhD Thesis, University of California, Santa Cruz
- Gorgas, J., Pedraz, S., Guzman, R., Cardiel, N., González, J. J., 1997, *ApJ*, 481, L19
- Grebel, E. K., 1999, in *The Stellar content of the Local Group*, IAU Symp. 192, ASP Conf. Series, eds. P. Whitelock & R. Cannon (astro-ph 9812443)
- Grebel, E. K., Guhathakurta, P., 1999, *ApJ*, 511, L101
- Grebel, E. K., 2000, in *The Evolution of Galaxies. I Observational Clues*, eds. J. M. Vilchez, G. Stasinska, E. Perez, Kluwer, Dordrecht (astro-ph 0011048)
- Gregg, M. D., 1991, in *The Stellar Populations of Galaxies*, IAU Symp. N.149, eds. Barbuy & Renzini, Kluwer, Dordrecht, p.426
- Greggio, L., & Renzini, A., 1990, *ApJ*, 364, 35
- Guzman, R., Lucey, J. R., Carter, D., Terlevich, R., J., 1992, *MNRAS*, 257, 187
- Held, E. V., Mould, J. R., 1994, *AnJ*, 107, 1307
- Jones, L. A., 1996, PhD Thesis, University of North Carolina, Chapel Hill
- Jones, L. A., Smail, I., Couch, W. J., 2000, *ApJ*, 528, 118
- Jorgensen, I., Franx, M., Kjaergaard, P., 1996, *MNRAS*, 280, 167
- Jorgensen, I., 1997, *MNRAS*, 288, 161
- Jorgensen, I., 1999, *MNRAS*, 306, 607
- Kauffmann, G., Charlot, S., 1998, *MNRAS*, 294, 705
- Kobayashi, C., Arimoto, N., 1999, *ApJ*, 527, 573
- Kodama, T., Arimoto, N., 1997, *A&A*, 321, 41

- Kodama T., Arimoto, N., Barger A. J., Aragon-Salamanca A., 1998, *A&A*, 334, 99
- Komiyama, Y. et al., 2001, *ApJ*, submitted (Paper I)
- Kuntschner, H., 1998, PhD Thesis, University of Durham, Durham
- Kuntschner, H., Davies, R. L., 1998, *MNRAS*, 295, L29
- Kuntschner, H., 2000, *MNRAS*, 315, 184
- Kuntschner, H., Lucey, J. R., Smith, R. J., Hudson, M. J., Davies, R. L., 2001, *MNRAS* in press (astro-ph 0011234)
- Larson, R. B., 1974, *MNRAS*, 166, 585
- Lee, H.-C., Yoon, S.-J., Lee, Y.-W., 2000, *AJ*, 120, 998
- Longhetti, M., PhD Thesis, University of Milano
- Longhetti, M., Bressan, A., Chiosi, C., Rampazzo, R., 2000, *A&A*, 353, 917
- Lucey, J. R., Guzman, R., Steel, J., Carter, D., 1997, *MNRAS*, 287, 899
- Maraston, C., 1998, *MNRAS*, 300, 872
- Maraston, C., Greggio, L., Thomas, D., 1999, in *The Evolution of Galaxies on Cosmological Timescales*, *A&SS* in press (astro-ph 9906088)
- Maraston, C., Thomas, D., 2000, *ApJ*, 541, 126
- Mateo, M., 1998, *ARAA*, 36, 435
- Mayer, L., Governato, F., Colpi, M., Moore, B., Quinn, T., Wadsley, J., Stadel, J., Lake, G., 2000, *ApJL* in press (astro-ph 0011041)
- Mehlert, D., Bender, R., Wegner, Saglia, R. P., G., 1998, in *Untangling Coma Berenices: a new vision of an old cluster*, p.107
- Mehlert, D., Saglia, R. P., Bender, R., Wegner, G., 2000, *A&AS*, 141, 449
- Mobasher, B., James, P. A., 2000, *MNRAS*, 316, 507
- Mobasher, B., Bridges, T. J., Carter, D., Poggianti, B. M., et al., *ApJ*, submitted (Paper II)
- Moore, B., Katz, N., Lake, G., Dressler, A., Oemler, A. Jr. 1996, *Nature*, 379, 613
- Moore, B., Lake, G., Katz, N., 1998, *ApJ*, 495, 139
- Murakami, I., Babul, A., 1999, *MNRAS*, 309, 161
- Peletier, R. F., 1989, PhD Thesis, Univ. of Groningen, NL
- Peterson, R. C., Caldwell, N., 1993, *AnJ*, 105, 1411
- Poggianti, B. M., Barbaro, G., 1997, *A&A* 325, 1025
- Poggianti, B. M., Smail, I., Dressler, A., Couch, W. J., Barger, A., Butcher, H., Ellis, R. S., Oemler, A., 1999, *ApJ*, 518, 576
- Rakos, K., Schombert, J., Maitzen, H. M., Prugovecki, S., Odell, A., 2001, *AJ*, in press (astro-ph 0012517)
- Rose, J. A., 1985, *AnJ*, 90, 1927
- Rose, J. A., 1994, *AnJ*, 107, 206
- Rose, J. A., Bower, R. G., Caldwell, N., Ellis, R. S., Sharples, R. M., Teague, P., 1994, *AJ*, 108, 2054
- Saglia, R. P., Mehlert, D., Bender, R., Wegner, G., 1999, in *From Stars to Galaxies to the Universe*, eds. Borner & Mo, p. 193
- Secker, J., 1996, *ApJ*, 469, L81

- Secker, J., Harris, W. E., Cote', P., Oke, J. B., 1997, in *A New Vision of an Old Cluster: Untangling Coma Berenices*, eds. Mazure A. et al. p. 115 (astro-ph 9709053)
- Silk, J., Wyse, R. F. G., Shields, G. A., 1987, *ApJ*, 322, L59
- Smail, I., Kuntschner, H., Kodama, T., Smith, G. P., Packham, C., Fruchter, A. S., Hook, R. N., 2001, *MNRAS* in press (astro-ph 0008160)
- Tantalo, R., Chiosi, C., Bressan, A., 1998, *A&A*, 333, 419
- Terlevich, R., Davies, R. L., Faber, S. M., Burstein, D., 1981, *MNRAS*, 196, 381
- Terlevich, A. I., Kuntschner, H., Bower, R. G., Caldwell, N., Sharples, R. M., 1999, *MNRAS*, 310, 445
- Thompson, L. A., Gregory, S. A., 1993, *AnJ*, 106, 2197
- Thuan, T. X., 1985, *ApJ*, 299, 881
- Trager, S. C., 1997, PhD Thesis, University of California, Santa Cruz
- Trager, S. C., Worthey, G., Faber, S. M., Burstein, D., González, J. J., 1998, *ApJS*, 116, 1
- Trager, S. C., Faber, S. M., Worthey, G., González, J. J., 2000a, *AnJ*, 119, 1645
- Trager, S. C., Faber, S. M., Worthey, G., González, J. J., 2000b, *AnJ*, 120, 165
- Vazdekis, A., Casuso, E., Peletier, R. F., Beckman, J. E., 1996, *ApJS*, 106, 307
- Vazdekis, A., Peletier, R. F., Beckman, J. E., Casuso, E., 1997, *ApJS*, 111, 203
- Vazdekis, A., Arimoto, N., 1999, *ApJ*, 525, 144
- Vazdekis, A., Salaris, M., Arimoto, N., Rose, J. A., 2001, *ApJ*, 549, in press (astro-ph 0011139)
- Weiss, A., Peletier, R. F., Matteucci, F., 1995, *A&A*, 296, 73
- White, S. D. W., Frenk, C. S., 1991, *ApJ*, 379, 52
- Worthey, G., Faber, S. M., González, J. J., 1992, *ApJ*, 398, 69
- Worthey, G., 1994, *ApJS*, 95, 107
- Worthey, G., Faber, S. M., González, J. J., Burstein, D., 1994, *ApJS*, 94, 687
- Worthey, G., Trager, S. C., Faber, S. M., 1995, in *Fresh Views on Elliptical Galaxies*, ASP Conf. Ser. vol. 86, eds. Buzzoni, Renzini, Serrano, Astron. Soc. Pac., S. Francisco, p.203
- Worthey, G., 1997, in *Star Formation Near and Far*, eds. Holt & Mundy, AIP Conf. Proc. vol. 393, p.525
- Worthey, G., Ottaviani, D. L., 1997, *ApJS*, 111, 377
- Worthey, G., 1998, *PASP*, 110, 888
- Ziegler, B., Bender, R., 1997, *MNRAS*, 291, 527
- Zinnecker, H., Cannon, R., Hawarden, T., MacGillivray, H., 1985, in *The Virgo cluster of galaxies*, eds. Richter & Binggeli (ESO, Garching), p.135

